Thermal Scanning Probe Lithography

Edoardo Albisetti[a], Annalisa Calo[b,c], Alessandra Zanut[d], Xiaouri Zhang[e], Giuseppe Maria de Peppo[d], Elisa Riedo[d*]

[a] Dipartimento di Fisica, Politecnico di Milano, Via Giuseppe Colombo 81, 20133 Milano, Italy

[b] University of Barcelona, C/Marti i Martí i Franquès, 1-11, 08028 Barcelona, Spain

[c] Institute for Bioengineering of Catalonia (IBEC), C/Baldiri Reixac 10-12, 08028 Barcelona, Spain

[d] Tandon School of Engineering, New York University, Brooklyn, New York 11201, United States

[e] Westlake University, Hangzhou, Zhejiang, China

[*] Corresponding authors: Elisa Riedo (elisa.riedo@nyu.edu)

Abstract

Thermal scanning probe lithography (tSPL) is a nanofabrication method for chemical and physical nanopatterning of a large variety of materials and polymer resists with a lateral resolution of 10 nm and a depth resolution of 1 nm. In this Primer, we describe the working principles of tSPL and highlight the characteristics that make it a powerful tool to locally and directly modify material properties in ambient conditions. We introduce the main features of tSPL, which can pattern surfaces by locally delivering heat using nano-sized thermal probes. We define the most critical patterning parameters in tSPL and describe post-patterning analysis of the obtained results. The main sources of reproducibility issues related to the probe and the sample, as well as the limitations of tSPL technique are discussed together with mitigation strategies. The applications of tSPL covered in this Primer include biomedicine, nanomagnetism, and nanoelectronics. In particular, we cover the fabrication of chemical gradients, tissue mimetic surfaces, waveguides for spin waves, and field effect transistors based on two-dimensional materials. Finally, we provide an outlook on new strategies that can improve tSPL for future research and fabrication of next generation devices.

(H1) Introduction

Nanolithography is the process used to fabricate nanostructures into a substrate, with defined geometrical shape and having a size, at least in one dimension, smaller than 1 μm. Often, nanolithography refers to both the fabrication of 3D structures and the patterning of a variety of properties in a material, such as patterning chemical, mechanical, electronic, and magnetic properties. The limitations of conventional nanolithography methods in terms of resolution, 3D patterning, and lack of flexibility for patterning material properties, have motivated the development of new fabrication techniques. For example, using conventional methods such as optical lithography and electron beam lithography, it is extremely challenging to pattern complex 3D structures with sub-100 nm resolution. Furthermore, chemical patterning at the nanoscale and direct magnetic patterning are impracticable with these two methods.

Thermal Scanning Probe Lithography (tSPL) is a unique method for rapid fabrication of nanostructures and nanodevices with extreme resolution (sub-10 nm lateral resolution) and high versatility[1]. It has been developed for researchers who need access to topographical and chemical patterning of arbitrary nanoscale geometries of non-conventional materials including polymer[2,3], 1D materials[4], 2D materials, magnetic materials[5], and biomolecules such as proteins and nucleic acids[6]. Even 3D nanopatterns can be fabricated in a single step and with the unmatched precision of 1 nm.

The main principle of tSPL consists in scaling down temperature-dependent processes occurring on the surface of a material to the size of few nanometers, i.e., the size of the contact region between a sharp probe and the surface touched by the probe itself. The technique works similarly to a scanning probe microscope (SPM) operated in contact mode, with the difference that the probe can be heated to reach very high temperatures, till around 800-1000°C. Using the hot probe, it is possible induce temperature-dependent processes that occur faster as temperature increases, like sublimation (the transformation of a solid into a gas), phase transitions and chemical reactions, making them occur in areas of the sample just tens of atoms or molecules wide. Additionally, with the probe in the cold state it is possible to image the surface of the sample, as in standard SPM.

A key component in a tSPL experiment is the thermally sensitive material, that can be a continuous thin film deposited over a surface (in this case, using the same terminology as for optical and electron beam lithography, this material will be called *resist* or *thermal resist*) or a single nanometric object that can be locally transformed using temperature. The other key

component in tSPL is the heatable nano probe that is scanned over the surface to locally activate the chemical and physical transformations in a large variety of substrate materials. tSPL can be exploited for topographical patterning of resists that evaporate or melt when they are heated by the hot nanoprobe[7,8], and for changing the chemistry of surfaces through local chemical reactions, here called *thermochemical reactions*. For example, tSPL has been successfully used to oxidize/reduce functionalized graphene with nanoscale precision[9], to activate reactive chemical groups on polymer surfaces[10], and to locally crystalize ceramic nanostructures[11]. A particular strength of tSPL is the precise control of the patterning parameters at the nanometer size scale and microsecond time scale. In fact, the tSPL probes contain integrated heaters which switch on and off with time constants between 5-100 μs[12], thus making possible a fast delivery of the thermal stimulus to the material under processing.

Additional characteristics of tSPL include (a) the *mask-less patterning* (**G**), i.e., tSPL is a direct writing technique that does not require a physical mask to protect the areas of the samples from unwanted transformations, (b) the *marker-less patterning* (**G**), i.e., tSPL does not require alignment markers, as the patterning area can be accessed safely (without inducing transformation during probe positioning) by using the probe in the cold state, (c) the *in situ* simultaneous writing and imaging using *closed loop lithography* (**G**), (d) the large areas patterning capability (10^4 cm^2), and (e) no need of vacuum environment. Nowadays, tSPL has reached a high level of technical maturity and dedicated tools, such as the commercial *NanoFrazor*, enable to perform reliable tSPL patterning using commercial polymer resists.

This article provides an overview of three particularly promising applications of tSPL, namely biomedicine, nanomagnetism, and nanoelectronics (Figure 1). These three topics are chosen for their relevance in different fields, i.e., tSPL has been used to produce reusable biomimetic surfaces[13] and functional biopatterns containing active enzymes and biomolecules[14], to fabricate high performance electrodes and nanomaterials with tailored electric properties for sub 10 nm electronics[15,16], and to produce magnetic patterns for efficient energy transport and wave-based computing[5,17]. Historical aspects of this technology as well as applications in other fields, such as optics will not be discussed in this Primer.

(H1) Experimentation

In this section the equipment and materials needed for carrying out tSPL will be discussed. The focus will be on the basic setup needed to perform tSPL patterning, the variations with respect to the basic setup allowing to address specific applications, the different material and sample preparations, and the main parameters affecting the patterning process and outcome. In particular, the differences and critical aspects of each implementation of the technique ranging from custom-made systems based on atomic force microscopy (AFM), to the more recent commercial tools dedicated to tSPL will be discussed for the three chosen applications, such as biomedicine, nanomagnetism, and nanoelectronics.

The equipment needed for performing tSPL comprises the heatable probe, a system for precisely scanning the probe on the sample surface, and the electronics allowing to heat the probe while scanning. The basic implementation (Figure 2a) involves the use of a customized AFM, in which the thermal probe is mounted, and the piezoelectric fine positioning is used for bringing the probe in contact with the surface and for scanning. The temperature of the thermal probe is controlled point-by-point while scanning by dedicated electronics.

(H2) Thermal probes

Heatable nanoscopic probes are the core technology enabling patterning by tSPL. The thermal probe is made up of a cantilever with a sharp probe at its end (see Figure 2b). The design of such cantilevers has evolved through the years, moving from commercial scanning probe microscopy (SPM) probes, which can be heated via laser irradiation[18], to more complex but practical designs with integrated Joule heaters[12]. This latter will be the focus of this Primer. Figure 2b shows a schematic of the thermal probe. It consists of special AFM cantilevers that can be heated controllably in the region located above the probe, the heater, via Joule heating **(G).** The heat then diffuses from the heater towards the apex of the probe, resulting in a highly localized hot spot of dimensions comparable to the apex curvature. U-shape heatable cantilevers are fabricated via a Silicon-on-Insulator (SOI) process[19], and possess a sharp probe with a radius of curvature ranging from 5 to 20 nm formed via oxidation sharpening **(G)**[20]. In order to obtain the conductive path and the heater region, the two cantilever legs are made of highly conductive silicon, while the heater region located above the probe is less conductive. This results in low resistivity legs and a high resistivity heater region, which spatially confines the Joule heating above the probe. The heater temperature T_H can be controlled electrically with a precision < 1°C, from room temperature up to

about 1200°C, with a heating/cooling time constant of a few μs[19,21]. It is worth noticing that prolonged high temperature heating close to the melting point of silicon (> 1000°C) can alter the doping profiles and ultimately damage the probe.

Thermal probes are used in SPM systems, in combination with the standard optical detection method, which uses the reflection of a laser beam bouncing off the cantilever for monitoring its deflection. More complex designs allowing a fully electrical detection[21] can be used with commercial tSPL setups. Such cantilevers feature two distinct heater regions, which can be addressed independently with minimal crosstalk. The first heater is located right above the probe and is responsible for heating the probe. The second heater is shifted with respect to the position of the probe and is used as a highly sensitive thermal probe of the cantilever-to-sample vertical distance. By recording the electrical resistance of the second heater while scanning the probe in contact with the sample, it is possible to build highly accurate SPM topographic maps of the surface, with a vertical resolution < 1 nm. The possibility to use the same probe for writing (when hot) and for inspecting the sample (when cold)[22] is the basis of the *in-situ* imaging capability of tSPL, which allows for extremely accurate stitching of multiple writing fields and overlay of multiple lithographic steps, with no need for additional markers[23,24].

(H2) Calibration and heat transport

(H3) Temperature

In most patterning applications, the probe is scanned in contact with the surface to transfer heat from the probe to the sample and produce highly localized reactions. In this process, the temperature is by far the most crucial parameter. For this reason, before patterning, a calibration of the probe temperature is performed by measuring the power dissipated by the heater as a function of the electrical current flowing in the cantilever (or the voltage applied). Since the cantilever self-deflects when heated, usually also the deflection signal is recorded during the calibration. The heater temperature can be measured experimentally via Raman or infrared microscopy[25] or, more conveniently, estimated directly from the dissipated power via a simple model[26]. At low temperatures, the electrical resistance of the heater increases with temperature due to the lower carrier mobility in silicon. However, as the temperature increases, the number of intrinsic carriers in silicon increases, until at a temperature T_i of approximately 560°C the thermally generated carriers dominate the cantilever resistance, which sharply decreases. Usually,

working below this threshold gives rise to a higher stability and a better control over the probe temperature and allows for longer thermal probe lifetimes. Figure 3a shows a schematic of the heat transport from the heater to the sample. It is worth noting, that the temperature at the probe-sample interface T_{int} is always lower than the heater temperature, due to thermal dissipation and imperfect heat transport within the probe and from the probe to sample. A simple model of the heat transport[12] allows to estimate T_{int} starting from the heater temperature T_H, knowing the thermal properties and geometry of probe and sample. However, due to the complex heat transport across surfaces with nanoscale roughness[27], accurately predicting T_{int} can be challenging. For this reason, for sake of reproducibility, usually T_H is specified in the experiments, instead of T_{int}. Importantly, the global sample temperature will also influence thermal dissipation. In fact, it is possible in general to reach higher T_{int} by heating the whole sample while performing tSPL (e.g., with a heatable sample holder).

(H3) Probe load

The probe load **(G)** is another crucial patterning parameter, which represents the force applied to the sample while scanning. As this force affects the probe-sample contact temperature and the quality of the pattern (sample damage, lateral resolution), it also needs to be calibrated. The calibration of the probe load is performed using the Hooke's law $F = kx$, where k is the spring constant **(G)** of the cantilever, and x is the cantilever deflection **(G)** in nm. The cantilever deflection depends on the vertical scanner position and in the case of thermal cantilevers it is also affected by the temperature in a process called thermal bending **(G)**. When customized SPM setups are used, the cantilever deflection is determined by the patterning setpoint plus the cantilever thermal bending at the patterning temperature, known as total cantilever deflection **(G)**. The reading of the setpoint is optical using the photodetector voltage and can be transformed to nm units by collecting a force curve on a hard surface as it is typically done in force spectroscopy experiments[28]. The thermal bending is also determined optically from the vertical photodetector voltage variations in function of the temperature in out-of-contact experiments.

In the case of dedicated commercial tools, the total cantilever deflection is determined by the capacitive voltage used to electrostatically bend the cantilever towards the sample surface plus the cantilever thermal bending. The load is determined as a function of the writing height, which is an operational parameter that can be adjusted by the operator during patterning and is a measure of

the probe-sample distance. The load L is defined as the writing height where the probe just contacts the sample and no patterning is achieved, minus the writing height during patterning at the same heater temperature and capacitive force [29]. The equation is the following:

$$L = k \cdot (h_{no\ pattern} - h_{pattern}) \quad \text{Eq. 1}$$

(H2) Setups for tSPL

There are two ways of performing tSPL, either using customized SPM setups or dedicated commercial tools. In the first case, shown schematically in Figure 2a, a SPM system is customized for allowing the controlled heating of the probe while scanning in contact mode across the sample. For doing so, an electronic circuitry is wired to the cantilever for providing a stable voltage/current to the heater, and it is either interfaced with the PC via DAQ or controlled manually. For patterning, the SPM control software or dedicated scripts (e.g., Matlab or Phyton) are used to raster-scan the probe in contact with the sample, while controlling the probe temperature in real-time. As in a conventional SPM topography, the vertical feedback loop keeps the cantilever deflection constant while scanning, while the in-plane closed-loop scanner precisely moves the probe or the sample in the plane of the film along arbitrary paths.

For each specific application, the basic setup is integrated with further equipment. In thermally assisted magnetic SPL (tam-SPL)[30], an external magnetic field is applied in correspondence of the sample, while performing tSPL, for patterning spin textures **(G)** in ferromagnetic thin films. For doing so, a rotatable permanent magnet placed in the vicinity of the sample is used to select the field orientation (in-plane or out-of-plane) and strength in correspondence of the sample. A schematic of the setup is shown in Figure 3b.

For applications ranging from biology to electronics, a controlled atmosphere may be needed. In the simplest configuration, inert gases such as N_2 and Ar or water vapor is flowed in the enclosed tSPL stage for controlling the humidity during patterning[15]. This control limits the formation of a water meniscus between the probe and the sample, which influences the spatial resolution and the heat transfer efficiency. More complex setups such as flow-through reactive-gas cells can be used for setting a controlled atmosphere[15]. As shown in Figure 3c, they consist of a gas cell with inlet and outlet tubes, that seals the environment around the sample and the tSPL scanning probe. Suitable gases can be flowed either directly through the cell or produced using a sealed flask of

solution, such as HCl and NaOH, where an inert gas is flowed for carrying the vapors inside the AFM gas cell.

Recently available commercial tSPL setups are in great part based on the principles of AFM-based tSPL. The most striking difference is the use of the electrical detection instead of the optical lever method for measuring the vertical positioning of the cantilever. In such systems, the sample is scanned in the plane, while the heated probe hovers above the sample at a fixed distance from the surface, and it is usually brought in contact intermittently "pixel-by-pixel" via electrostatic forces between the cantilever and the sample.

(H2) Samples and material preparation

Given the broad range of applications, the sample preparation techniques vary widely. Here, the focus will be on the sample preparation for the three applications, namely biomedicine, nanomagnetism, and nanoelectronics.

(H3) Biomedicine

In addition to polyphthalaldeyde (PPA), which is a commercial resist that sublimates upon temperature exposure[31] and is widely used for many tSPL-based applications, researchers have also developed a poly((tetrahydropyran-2-yl N-(2 methacryloxyethyl) carbamate)-b-(methyl 4-(3-methacryloyloxypropoxy) cinnamate)) (PMCC) resist, which can be chemically and topographically modified. PMCC can be spin coated on different substrates, including silicon, silicon oxide or transparent indium tin oxide (ITO) glass. PMCC display characteristics that make it an ideal resist for biomedical applications of tSPL, including biocompatibility, stability in wet hydrophilic environments, and ability to be patterned chemically by local heating, which enable the carving and simultaneous chemical deprotectation of amine or carboxylic groups on the polymer resist surface with nanoscale precision[6,14,29,32-34]. This is possible thanks to a chemical conversion occurring in methacrylate block-copolymers such as the PMCC resist by applying a specific range of temperature below the glass transition temperature of the material. To trigger a chemical conversion, the polymer film should possess a high glass transition temperature to improve stability and avoid softening of the film, which could also lead to probe contamination.

Mechanically stable PMCC thin films are obtained by spin-coating a polymer solution in organic solvents (typically 2.5 mg/mL solutions in chloroform or cyclohexanone, with typical spinning

conditions of 1500 rpm for 60 s)[29,34], followed by UV crosslinking or backing at 50°C. These conditions guarantee optimal substrate attachment and film thickness around 20-30 nm. Typical probe temperatures at which the deprotection reaction **(G)** range between 160 and 240°C. The local thermal patterning induces a temperature-dependent change in the chemical functionality of the surface (ester to carboxylic acid, or carbamate to amine), at speeds higher than 1 mm/s and features as small as 10 nm. In particular, at temperatures around 150°C the formation of amine groups is the thermodynamically favored process, while at T > 200°C the formation of carboxylic acid is the most stable reaction product[14]. The final surface concentration of exposed reactive groups is controlled by the temperature profile at the probe-surface interface, the integrated time of exposure, and the activation energy required for the reaction. This surface concentration can be tailored to an optimum value, from low to 100% coverage[33], depending on the specific application. The control of the density of functional groups at the resist surface is the base of chemical gradients patterning (see the application section) and can be exploited for functionalizing the polymer resist with different kinds of biomolecules.

PMCC has been optimized to enable the patterning of biomimetic surfaces for cell culture studies. To mimic the complexity of the tissue microenvironment on a cell culture substrate, the fabrication process must produce the topographical information of the tissue microenvironment with nanometer precision and must be highly effective in relation to its production cost. The PMCC resist was shown to support the culture of human-induced mesenchymal stem cells similarly to standard polystyrene tissue culture plastic[13].

Moreover, a novel protocol for tSPL sample preparation that involves the use of plasma polymerization of allylamine (ALA) to improve the immobilization of the PPA thermolabile resist on the substrate has been implemented[35]. This treatment helps to avoid PPA detachment from silicon substrates in aqueous solution to enable cells culture. In the case of PPA, mechanical stable films are fabricated on silicon substrate on which ALA is deposited by plasma polymerization followed by PPA spin coating to achieve 100 nm thick films (4000 rpm for 60 s at ambient conditions) and a baking step at 90 °C for 3 min to remove the residual solvent. This strategy has been exploited to replicate the nanoscale morphology of a generalized tendon pattern in a film of PPA polymer stabilized on a silicon wafer inducing formation of cell focal adhesions similarly to native tendon sections.

Despite the improvements on the biocompatibility side, the main drawback of tSPL for biomedical applications remains the limited throughput, which makes it difficult to nanopattern large areas rapidly and cost-effectively. This aspect is addressed later in the chapter "Critical Parameters".

(H3) NanoMagnetism

Patterning spin textures via tam-SPL requires the use of magnetic heterostructures displaying the exchange bias effect **(G)**[36]. By performing tamSPL with a temperature above its blocking temperature **(G)**, while applying an external magnetic field, the magnetization pinning direction is locally re-set along the external field direction.

The magnetic thin film heterostructures are grown via magnetron sputtering, usually on Si, Si/SiO_2, glass substrates, or SiN membranes for allowing experiments in transmission. A thin capping layer is used for protecting the structure from the external environment. Their magnetic properties are then characterized via standard bulk techniques such as Vibrating Sample Magnetometry (VSM) or Magneto-Optical Kerr Effect (MOKE)[37]. Before patterning, a uniform magnetization direction is set across the whole sample by heating and cooling down the system in presence of an external magnetic field. The simplest magnetic systems used in tam-SPL is a ferromagnet/antiferromagnet FM/AF bilayer characterized by a magnetization which lays within the plane of the film, and that can be set via tamSPL along an arbitrary in-plane direction. More complex systems are the synthetic antiferromagnets, consisting of a FM/spacer/FM/AF, where the two ferromagnetic layers are coupled antiferromagnetically by the presence of a thin nonmagnetic spacer[38]. In general, for patterning spin textures via tamSPL, it is required that the exchange bias effect is strong enough to set the magnetization orientation at remanence, i.e. when no external magnetic fields are applied.

The most critical aspect in view of tamSPL, is making sure that the blocking temperature of the system lays within the reachable probe-sample interface temperature range. Two possible strategies can be pursued: lowering the blocking temperature, e.g., by tuning the antiferromagnetic layer thickness or composition[39], or lowering the thermal conductivity of the sample by growing it on thermally insulating substrates. The probe-sample interface temperature can be increased also by heating the whole substrate while performing tamSPL. In this case the "global" heating temperature should be kept lower than the blocking temperature.

(H3) NanoElectronics

The core advantage of tSPL is to generate local heat distributions within a confined nanoscale region. Therefore, smart control of this nanoscale heating enables a wide range of applications of tSPL in nanoelectronics.

First, lithography through tSPL utilizes the ultraclean evaporation process of a thermal resist (e.g., PPA) when heated at around 185°C. In addition, a combination of various polymer stacks under the thermally sensitive resist can facilitate the pattern transfer from the thermal resist to substrates of interests. Therefore, polymer stacks can be purposedly designed according to specific applications and needs. For instance, PPA/polymethylglutarimide (PMGI) polymer stacks can be used to pattern high performing electrodes on 2D semiconductors[16]. In this case, a thin film (20 nm) of PPA is deposited over a 150 nm thin film of PMGI by spin coating it on a clean SiO_2/Si substrate pretreated with hexamethyldisilazane (HDMS). After tSPL patterning and PPA evaporation, PMGI is etched in tetramethylammonium hydroxide (TMAH) to form the essential undercut. Finally, metal evaporation and resist lift off via the solvent (the commercial solvent is called *remover PG*) produce the final electrode structures, see Figure 8. It must be noticed that these steps can be repeated after the fabrication of bottom gate electrodes to obtain the top gate configuration[16]. The tSPL process produces high performing electrodes due to the ultraclean surface after the tSPL process, and the doped contact area obtained after developing PMGI. Both effects give rise to a low Schottky barrier between the metal contact and the substrate **(G)**. Moreover, tSPL offers *in-situ* observation of the 2D semiconductors coated with the polymer stack, enabling mask-less and marker-less lithography advantages.

Secondly, besides the lift-off process for electrodes, lithography through tSPL is compatible with typical pattern transfer techniques, such as etching, for transferring both 2D and 3D nanostructures, as well as molding and assembly. For instance, arbitrary shape structures can be defined on transition metal dichalcogenides (TMDC) monolayers via plasma dry etching **(G)** following the tSPL lithography. The same polymer stack (20 nm PPA and 150 nm PMGI) is deposited on TMDC flakes firstly. The unwanted areas on TMDC flakes can be defined and exposed through tSPL lithography and TMAH etching. Subsequently, the selected regions on TMDC flakes can be etched away, leading to the well-defined channels and hence the universal platform for integrated circuits on TMDC materials. Moreover, tSPL lithography is readily for a

wide range of materials such as graphene and WSe_2[40], and for the scalable and cost-effective nanofabrication method, providing indispensable attributes for nanoelectronic applications.

Thirdly, tSPL can be used to directly pattern certain thermally sensitive materials for various material modifications, such as phase transition, doping, cutting, crystallization, oxidation, reduction, functionalization, *et cetera*. For example, 2D semiconductors can be effectively doped by tSPL owing to the large number of vacancies/defects. The tSPL setup needs to be modified with an environmental chamber and special gases needs to be introduced depending on various doping polarities or levels. Typically, gases can be introduced in the tSPL system using a small liquid cell with an inlet and an outlet and flowing inside it a gas or the vapor generated from a solution. Commercial tSPL setups allow the control of the patterning environment with pure, inert gases, such as N_2. Eventually, the doping of 2D semiconductors can be precisely tailored via adaptive controlling of the temperature, the speed, loading force, and gas environment of the tSPL[15]. 2D transition metal dichalcogenide MoS2, for example, can be chemically modified (p-defects) in HCl atmosphere flowing an inert N_2 gas (flow rate: 60 mL/min) inside a HCl solution ((HCl) = 2.4 M) at probe temperature over 600°C. In N_2 atmosphere alone, n-type defects can be produced at probe temperature ranging from 900 to 1100°C. To allow for such modifications, critical parameters are the patterning speed, which needs to be kept low (from 0.2 to 0.02 μms^{-1}), and the load, which can reach values as high as few μN. As another example, poorly conductive epitaxial graphene oxide 2D layers can be locally reduced to obtain graphene-like nanostructures exhibiting enhanced electrical conductivity across order of magnitude by locally heating at temperatures above 800°C, and using writing speeds of 0.2 μms^{-1} and loads of 120 nN[9].

In conclusion, the polymer stacks and the suitable materials need to be carefully designed for the use of tSPL in nanoelectronics in terms of lithography and material modifications.

2.5 Data output

(H2) Critical parameters

Most of the tSPL parameters strongly influencing the patterning outcome are in common to all applications and can be divided in two categories, such as the ones related to the patterning process, which are the heater temperature, probe geometry, probe load and patterning speed, and the ones related to the sample used, i.e., the thermal conductivity, the thickness, the activation energy of the thermochemical reaction. Among these, the most critical is the heater temperature T_H, which

is directly linked to the probe-sample interface temperature T_{int}, as explained above. In general terms, the dependence of the patterning outcome with T_H goes through three phases. At low T_H, no reaction is promoted, usually because the thermal energy is below the activation energy required to trigger the reaction. At higher T_H, above this threshold, the reaction products generally increase with temperature and a further increase to higher T_H triggers unwanted reactions leading to the degradation of the substrate/sample. The heater temperature can be controlled from room temperature up to about 1200°C, with a precision < 1°C.

The probe geometry and probe load both influence the heat transport from the heater to the interface. A sharper probe, i.e., with smaller radius and lower cone angle, leads to lower T_{int} due to the reduced heat transport associated with phonon scattering at the probe boundaries, but conversely allows a higher spatial resolution due to the more confined thermal profile. Ultrasharp tSPL probes possess a radius < 5 nm. Increasing the probe load increases the effective contact area between the probe and the sample, leading to higher T_{int} and lower spatial resolution.

The patterning speed (or conversely, the heating time of each pixel) generally has a lower impact than the patterning temperature on the reaction products but can nevertheless strongly influence the outcome when the characteristic timescales of the reactions are comparable with the typical pixel time (e.g., in the case of Arrhenius thermochemical reactions). Generally, the higher the patterning speed (or lower pixel time), the lower the reaction products.

The thermal conductivity and thickness of the substrate and film both influence the T_{int}. Higher thermal conductivity leads to more efficient heat dissipation and therefore to a lower T_{int}, and a higher spatial confinement of the thermal profile within the film. Therefore, generally highly conductive substrates/films lead to lower T_{int} and higher spatial resolution, and *vice versa*. Regarding the film thickness, the thicker is the film, the lower is the influence of the substrate on the overall thermal conductivity of the sample. For a film roughly ten times thicker than the probe radius, the influence of the substrate is negligible[41].

The activation energy of the reaction is threshold thermal energy required to trigger the reaction. In case of thermochemical reactions, the activation energy directly controls the reaction rate, and therefore the reaction products, so that higher activation energy requires either higher temperature or longer time for completing the reaction. In physical phenomena, such as in the case of purely magnetic or electronic phase transitions, the activation energy takes on the broader meaning of

threshold temperature. In these cases, generally, the heating time has a minor impact on the outcome, due to their much faster timescales.

While such parameters are common to all techniques, some effects and parameters are typical of specific applications, as described in detail here.

(H3) Biomedicine

Recently, a new platform named bio-tSPL has been developed for reproducing biological tissues in polymer resists (see Figure 6). Bio-tSPL involves the pixilation of a biological tissue image, generated via high-resolution imaging methods, and then its replication by assigning at each grey level of individual pixels a specific height level. The main drawback of tSPL techniques, including tSPL for applications in biomedicine, is the limited throughput associated with the serial writing process, the low writing speed, as well as the high cost of large-scale patterning.

Using tSPL, researchers have patterned complex quasi-3D tissue microenvironments with high fidelity and resolution[13]. However, due to probe contamination occurring during patterning, the quality and resolution of the biological tissue replicas decrease quite dramatically over time, eventually impeding further patterning completely. Therefore, to pattern larger areas required for biomedical applications, it would be required to change the thermal probe thousands of times. One solution to this issue is to adopt a threshold filtering strategy of the input image to increase the number of 0-level pixels that do not require writing (and hence the probe-surface contact), therefore reducing probe contamination while increasing its durability. This reduction has a major impact in decreasing the costs and increasing the throughput since changing the probe requires time. Another strategy to increase throughput is using a parallel process, i.e., many heatable cantilevers working in parallel[42].

To further reduce the costs related to the large number of thermal probes needed for large-scale fabrication of tissue replicas, a probe washing procedure can be introduced, based on cleaning the probe in a specific solvent (usually the solvent present in the resist solution). Liu *et al.* demonstrated the ability to clean the probe and to recover high-resolution writing of bone replica patterns[13]. Furthermore, to improve the patterning speed while maintaining a faithful pattern reproduction, pixel dwell-time, t_{dwell} (40 µs-70 µs) and pixel size, d_{pixel} (12 nm – 20 nm) are key parameters to be optimized (**G**). Pixel dwell-time and pixel size correspond to the time interval and the distance between two adjacent writing pixels, respectively. While shorter pixel dwell-times

and larger pixel sizes increase writing speed, it should be considered that large pixel size influences the pattern resolution especially for sub-20 nm structures. Once all settings are optimized, it is possible to calculate the real throughput for patterning mm^2 areas by taking into consideration also the extra time required to invert the trajectory of the probe at the end of each patterning line, which is estimated to be 0.05 s per turnaround, using the following formula:

$$\frac{1}{\text{throughput } (\text{mm}^2/\text{h})} = \frac{1\ \text{mm}^2}{d_{pixel}^2} \times\ t_{dwell} + n_t \times t_{turnaround} + t_{change} \times n_{probes} \quad (1)$$

Where n_t is the number of turnarounds per mm^2, t_{change} is the time spent to replace each of the thermal probes required to pattern 1 mm^2, n_{probes} is the total number of thermal probes per mm^2. This latter parameter depends on the writing setting as well as on the polymer resist used for fabrication. Using a non-commercial tSPL system, speeds of 0.05 $mm^2\ h^{-1}$ have been demonstrated for areas smaller than 174 μm^2 (i.e., for a single probe), and taking into account the turnaround time[43]. However, the real throughput to pattern 1 mm^2 must include the third term in the equation above, which decreases the writing speed due to probe-change time, depending on the resist material used during the fabrication.

NanoMagnetism

In tamSPL, the magnetic field strength should be high enough to fully saturate the magnetization of the ferromagnetic layer. Depending on the sample type it can range from a few mT up to a few hundred mT. The field direction determines the direction of the magnetization within the pattern. Regarding the patterning temperature, when T_{int} is higher than the blocking temperature, the exchange bias is fully rewritten in the direction of the field. However, by heating close to the blocking temperature, it is usually possible to precisely tune the exchange bias strength.

(H3) NanoElectronics

For lithography via tSPL, the polymer stack needs to be carefully designed and prepared. The first PPA layer, serving as the thermal sensitive resist, is supposed to be thin enough for the thermally heated probe to pattern without contaminations or residuals, and strong enough to protect the nanostructures against the subsequent etching process. In the meanwhile, the thickness of the

sacrificing PMGI layer is highly dependent on the metal thickness of the lift-off process and the minimal feature size of the etching process, respectively. The typical thickness of PPA layer is around 15 nm for tSPL-based lithography, and the PMGI is around 210 nm and 70 nm for the lift-off and etching process, respectively.

For reduction/doping via tSPL, a key point is the prolonged contact between the thermal probe and the materials using a probe temperature above the threshold temperature. Therefore, a group of parameters needs to be precisely tailored including scan rate, probe set point, temperature, and gas flow rate. It should be noted that there is more than one combination of parameters that can produce effective interactions.

(H1) Results

(H2) Biomedicine

For applications in biomedicine, tSPL is used in combination with polymer resists that can be topographically and chemically modified, either independently or simultaneously, to fabricate patterns with high topographical and chemical complexity. Following patterning, the resulting topography is visualized either using the *in-situ* imaging capability of the NanoFrazor, during which a cold tSPL probe profiles the polymer resist surface, or via traditional SPM imaging. On the other hand, to visualize the programmed gradient of reactive groups on the polymer surface, friction force microscopy together with fluorescence optical microscopy can be used. Here, the deprotected amines are fluorescently labeled using a N-Hydroxysuccinimide (NHS) fluorescent dye and imaged with fluorescence microscopy[44]. Another labelling strategy involves the immobilization of negatively charged sulfonated Alexa-488 labeled enzymes through electrostatic interaction in aqueous environment (pH $\sim$ 7 and 7.4 for washing) between the charged sulfonated Alexa-488 labeled enzymes and the positively charged amine groups on the patterns[29] (Figure 5). Using Alexa-488 labeled enzymes, researchers have predicted the density of amine groups on the surface by using an Arrhenius model for the thermally activated chemical reaction, which is influenced by the probe-surface interaction temperature, the time of exposure, and the activation energy of amine deprotection. Since this is a unimolecular reaction, it can be modelled using first-order chemical kinetics equations:

$$\frac{dN_{Amine}}{dt} = k(N^0_{Amine} - N_{Amine}), \text{ with } k = A \exp\left(\frac{-E_a}{RT}\right) \qquad \text{Equation 1}$$

where N_{Amine} is the amine density in the patterned areas, which for low temperatures can be considered to be proportional to the density of sulfonated molecules specifically and electrostatically immobilized at the amine groups, while N^0_{Amine} is the maximum achievable amine density, *t* is the time, *k* is the rate constant, *A* is the Arrhenius constant, *R* is the gas constant, 8.3145 J/mol·K, *T* is the temperature at probe-polymer contact, and E_a is the activation energy of the reaction. Solving for N_{Amine} the following equation is obtained:

$$N_{Amine} = N^0_{Amine}\left(1 - \exp\left(-At_d \exp\left(\frac{-E_a}{RT}\right)\right)\right) \qquad \text{Equation 2}$$

where t_d is the probe-polymer dwelling time, calculated to be 1.4×10^{-4} s for a patterning speed of 0.2 mm/s, and N^0_{Amine} corresponds to the maximum density of deprotected amine groups. The density and maximum density of amines are inferred from fluorescence measurements and are proportional to the fluorescence intensity.

(H2) Nanomagnetism

TamSPL[5] allows to write magnetic textures such as magnetic domains and domain walls in continuous magnetic films, without producing chemical, topographical or structural changes to the sample. The characterization techniques can be divided into static techniques suited for visualizing the magnetic domain structure, and "dynamic" techniques able to study the magnetization dynamics.

The static characterization requires to measure the magnetic properties with nanoscale resolution. Magnetic Force Microscopy (MFM)[45] is the method of choice because it allows to directly characterize the magnetic domain structure with sub-50 nm spatial resolution. By performing MFM while applying a variable external magnetic field, it is possible to study the nucleation and field evolution of the textures. The main drawback of MFM is related to the fact that the oscillating magnetic probe, which is scanned close to the surface, can influence and modify the magnetic domain structure. An example of this is the typical domain wall "roughness", which is caused by the magnetic probe reorienting the magnetization of the domain wall while scanning. Different

types of magnetic probes such as low-coercivity probes allow to reduce these unwanted effects. Magneto-Optical methods, such as the Magneto Optical Kerr Effect (MOKE)[46] or Faraday Effect allow to locally probe the magnetization by analyzing the change in polarization of reflected or transmitted light, respectively. In order to achieve the high spatial resolution needed for visualizing the patterns, it is possible to either raster scan a focused laser (Micro-Focused MOKE) or use a microscope in combination with a CCD camera (Kerr Microscopy) for directly acquiring the whole magnetic image. Optical techniques allow lower acquisition times and reduced interaction with the sample, with respect to MFM, but their spatial resolution is limited by diffraction usually around 250 nm.

Imaging the magnetization dynamics **(G)** requires first to excite it. In most cases, this is done by an oscillating external magnetic field in the GHz frequency range, provided for example by a coplanar waveguide patterned onto the sample. Second, one must use specific techniques able to combine high temporal and spatial resolution. These methods include time-resolved MOKE and X-Ray microscopy. In the first case, femtosecond laser pulses are synchronized with the excitation signal, and focused on the sample. The polarization of the reflected beam is then analyzed for extracting the magnetic information[47]. In the second case, X-Ray Magnetic Circular Dichroism (XCMD), i.e., the different absorption rate of circularly polarized X-Rays by magnetic materials depending on the direction of the magnetization, allows to obtain time-resolved images with extreme spatial resolution, down to a few nm[48]. While Time-resolved MOKE can be performed in table-top systems, X-Ray microscopy requires bright monochromatic X-Ray sources such as synchrotrons. A last technique which is particularly suited for studying spin waves in magnetic nanostructures, with high spatial resolution is Micro-Focused Brillouin Light Scattering (μBLS). Here, incident visible photons interact with the spin waves **(G)** propagating in the material, are scattered inelastically and analyzed for extracting information on the dispersion and intensity of the spin waves.

(H3) Nanoelectronics

tSPL can be used to fabricate high-quality metal contacts on 2D materials with high reproducibility [15,16,40]. tSPL has a wide range of advantages compared to conventional lithography methods (e.g.,

electron beam lithography or optical lithography), such as the possibility to work in ambient conditions without the need for high vacuum, ultrashort channel fabrication (14 nm length), *in-situ* sample imaging, and closed-loop patterning with an overlay accuracy better than 5 nm. The tSPL approach has also been used to fabricate top-gated and back-gated FETs on one layer (1L) MoS_2, 1L Wse_2 and graphene. By eliminating resist contamination, as well as damage from either electrons or photons, MoS_2 FETs show linear I–V curves even at low temperatures, record low Schottky barrier heights (~ 0 mV), record high on/off ratios (10^{10}) and exceptionally low subthreshold swing (64 mV per decade). The graphene FETs fabricated using tSPL exhibit a relatively low specific contact resistance of 600 Ω·μm and a symmetric conductance at the Dirac point without the use of any contact engineering strategy. In addition, tSPL is compatible with standard etching procedures and could potentially be pushed to single-digit nm spatial resolution and, by mulprobelexing with thermal nanoprobe arrays, to higher throughput. The approach could thus lead to low-cost, no vacuum, one-step industrial metal nanomanufacturing.

(H3) Defect engineering

To realize the spatial defects engineering of emerging 2D materials (such as MoS_2), the environment control of the tSPL patterning process is required and achieved via the integration of a flow-through reactive gas cell. For instance, the doping polarity MoS_2 of can be easily tuned between p-type and n-type on demand, depending on the used gases. Consequently, various functional nanoelectronic devices have been demonstrated including field effect trasnistors, phototransistors and p-n junctions precise sub-μm spatial control, and a rectification ratio of over 10^{415}. To assess the output of the tSPL process for nanoelectronics applications, independent measurements must be performed *post patterning*. These measurements include X-Ray photoelectron spectroscopy (XPS) (with spatial resolution in the hundreds of micrometer range), Kelvin Probe Force microscopy (KPFM), friction force microscopy and Raman spectroscopy (with spatial resolution of less than 5 micrometers) and High Angle Annular Dark Field Scanning Transmission Electron Microscopy (HAADF-STEM) (with atomic resolution), as well as the material response once tested in devices, like field effect transistors (FETs) or other electronic transport measurements. AFM topography can be used to assess the size of the smallest patterning lines or the presence of topographic variations after the transformation of functional materials. KPFM has been used in both amplitude and frequency modulation modes (see the Related Links

section), also in conjunction with XPS, to assess work function variations due to defect production in 2D materials after patterning. Work function variations are inferred from the contact potential difference in patterned areas compared to the surrounding areas of the same 2D material flake which has not been in contact with the hot tSPL probe (KPFM) in locally heated samples and from the shifts of the Mo 3d core levels, S 2p core levels and valence band maximum (VBM) in XPS spectra of globally heated MoS_2 samples. Raman spectroscopy is also a valuable and fast tool to assess p/n character of the defects produces by tSPL. Similarly to KPFM, it can be used to assess difference between tSPL patterned and non-patterned areas of the same flake, because the size of the Raman laser is smaller than 5 micrometers. In the literature, it has been demonstrated that a blue/red shift of the Raman active A_{1g} peak of MoS_2 indicates p/n doping, respectively, while a lowering or an enlargement of the E^1_{2g} A_{1g} peaks is associated to defects formation that break the crystalline symmetry and order of the 2D material[49,50]. FETs can be used to characterize p-n junctions fabricated by tSPL and to test the p-n character of the patterned region through the shift of the threshold voltage.

(H1) Applications

tSPL is characterized by unique features that make it possible to perform tasks not achievable by standard lithographic techniques, and also enable completely new routes in the production and manipulation of advanced materials, thanks to its versatility, and the gentle processing mechanism, based on the controlled heat activation of surfaces at the nanoscale. In the context of standard lithographic processes, tSPL can fabricate different types of devices, similarly to those fabricated by EBL. Nevertheless, it is also possible to obtain greyscale lithography with nanometer resolution together with an unprecedented lateral resolution of single features (lines, dots) < 10 nm[16,29]. This advanced precision in tSPL is due to the lack of proximity effects, that provoke the lateral spread of electrons to adjacent pixels due to scattering effects inside the non-irradiated resist and the substrate when electron beams are used. It must be noticed that EBL resists for high resolution generally require high electron doses and this fact limits the patterning speed by EBL when high resolution needs to be obtained. Instead, the tSPL process typically uses resist that rapidly (1 ms) sublimate upon thermal contact, thus it does not require chemical developing after patterning, a process that in EBL patterning can also affect resolution[51,52]. An additional advantage of tSPL sublimating resists, like the PPA, is that it makes the fabrication process very clean, i.e., no resist

residuals are left on the substrate after patterning. In contrast, PMMA, a commonly used resist in EBL, is generally hard to be completely removed by developers[16].

Finally, a unique feature of tSPL technology is the capability of *in-situ* imaging (low temperature imaging), which is very useful to immediately check the patterning results without any damage to the surface and the resist film. Also buried materials under the resist can be imaged, thus allowing for the accurate and easy alignment of structures, like electrodes, on 1D or 2D materials[53].

Alternative standard lithographic techniques, as the greyscale optical lithography, even if faster, does not offer a resolution comparable to tSPL. Successful examples of 3D greyscale structures by tSPL include 3D pattern transfer of nanometric features on hard surfaces, like silicon[2,54], holograms and gratings for the generation of optical signals with subwavelength resolution for applications in optics[55,56].

Completely new routes can be explored that involve materials transformations at the nanoscale by using the versatility of the tSPL technique. TSPL, in fact, does not require vacuum, it is compatible with ambient conditions, including glovebox, and can integrate different gases for activating thermochemical reactions. Plenty of synthetic chemistry routes, normally happening in solution, could thus be tested on surfaces with a high degree of parameters control (temperature, load, size, degree of conversion)[6]. Such versatility has been successfully exploited for the generation of chemical gradients[32], to grow ferroelectric nanocrystals[11] or to quench a supramolecular polymer[57]. In all these applications the process is completely clean (only the material in contact to the very end of the probe is modified). Additionally, heat does not spread out of the patterned areas, thus unwanted effects, such as defects creation and chemical bonds breakage, do not happen either in the substrate or in buried structures covered by the thermal resist, contrarily to what happens with more destructive electron beams.

(H2) tSPL for biomedical applications

Over the past decade, tSPL has been exploited for various biomedical applications by harnessing its capability to fabricate, position, and interconnect nanoscale structures and objects, such biological molecules, onto thermally sensitive polymer resists with different properties and chemistry. In this context, tSPL overcomes the limitations of conventional lithographic techniques associated with limited resolution, high cost, and lack of flexibility for soft and novel materials[16].

For example, by exploiting the closed loop lithography scheme of tSPL, the patterning depth in a polymer resist can be controlled to 1 nm precision, which is less than the linear dimension of a single resist molecule.

A similar control was obtained for the degree of chemical functionalization in a thermally sensitive polymer, thus obtaining chemical gradients that can be fluorescently labelled for further visualization[32,33].

The process for the fabrication of chemical gradients starts with the polymer film deposition. PMCC is a versatile polymer that can be deposited as thin film on different substrates, like glass and Silicon. Films with thickness ranging from 20 to 150 nm have been fabricated controlling the spinning conditions[34]. For bio-applications, typical film thickness of 20 nm is used, obtained by spinning at 1500 rpm for 1 minute. Once the film is produced, tSPL patterning is performed on areas ranging from tens of micrometers till less than 10x10 nm^2 in ambient conditions and at room T, using controlled conditions (dissipated power/T, load, and speed). Practical patterning conditions include load in the range 10-50 nN[14], speed in the range 0.1-1 mm/s, and dissipated power from 6-11 mW, corresponding to a T = 140-260°C. A typical workflow for fabricating chemical gradients is based on several steps (see Figure 6), such the uptake of a user defined greyscale image that is intended to be replicated, the construction of a calibration curve of relative concentration versus power/temperature based on the Arrhenius model (see Equations 1 and 2), the creation of the power map necessary to visualize the greyscale image with appropriate contrast, and the patterning with the thermal cantilever.

After tSPL patterning, chemical gradient images, such as the Monna Lisa replica shown in Figure 6f, can be visualized by fluorescence microscopy, using a covalently or electrostatically bound dye molecule. This step is achieved by simply dipping the pattern in the dye solution (100 μL of 25 nM NHS-DyLight 633 diluted in dimethylsulfoxide DMSO for 1 hour or 100 μL of 100 nM Alexa488 in water for 45 min are typical conditions for the attachment of commercial dyes)[14,33]. Another visualization technique is the AFM topography (chemical patterns are generally associated to topographic variations) and friction force microscopy for compositional mapping[33]. The chemical gradients can finally be used to attach enzymes or to build complex constructs via protein-protein specific interactions, such as the biotin-streptavidin interaction. For enzyme attachment, the pattern can be dipped in Alexa488-Thermolysin conjugate in water (at a concentration of 1 mg/mL) for 1 hour. For building biotin-streptavidin constructs, the pattern can

be first dipped in 1μM NHS-biotin in DMSO for 1 hour, then for 30 min in a 100 nM DyLight®633-streptavidin solution in phosphate-buffered saline (PBS) solution. Subsequent steps include the addition of biotinylated laminin and rabbit anti-laminin primary antibody followed by anti-rabbit secondary antibody for visualization through immunofluorescence[32]. After each functionalization step, the substrate must be washed with deionized water and dried with N_2.

The mechanism for the generation of chemical gradients is a thermally induced deprotection reaction, forming reactive groups, such as amines, at the surface of the polymer film. The exposed amine groups can then be selectively and covalently functionalized. By varying a spatiotemporal temperature profile at the surface, the chemical concentration gradients can be translated into a gradient of biomolecules, proteins, and enzymes with potential applications in diverse research fields, including bioengineering and biosensing.

In particular, fluorescent biotin-streptavidin patterns and biotinylated protein-antibody constructs can serve as substrates for cell deposition[32]. Fluorescent enzyme gradients can be employed as platforms for catalysis and enzyme-mediated supramolecular chemistry[14]. These patterns can eventually be exploited to create nanoarrays of nano-objects with features smaller than 10 nm, including reactive molecules with biological activity such as proteins, RNA, and DNA using standard functionalization methods. The development of protein chips with single-molecule detection capability enables the construction of new biosensing devices, and can assist in fundamental studies of biological interactions, such as the formation of neurological synapses and cell focal contacts.

An advantage of tSPL is the capability for multiple patterning routes to be applied on the same sample, such that unpatterned areas of the polymer remain unaffected in a certain fabrication step, allowing subsequent cycles of tSPL patterning to unmask additional reactive groups on distinct areas of the sample. This iterative approach allows for the fabrication of surfaces with multiple orthogonal functionalities, i.e., patterns of thiols, maleimides, aldehydes or biotins can be obtained on a single surface[34], each one with their own well-defined and independent patterns[10,29,32,33]. The patterned chemical functionalities can be then used to produce *ad hoc* arrays of multiple types of enzymes[14].

Recently, tSPL has been exploited to reproduce the nanoscale complexity of biological tissues, with potential for tissue engineering and regenerative medicine applications. For example, this strategy has been exploited to replicate the nanoscale morphology of a generalized tendon pattern

in a film of PPA polymer stabilized on a silicon wafer inducing formation of cell focal adhesions similarly to native tendon sections[35].

In a different study, smart software and post-patterning procedures have been introduced to replicate the complex quasi-3D morphology of the bone tissue into a film of the PMCC polymer, which is biocompatible and can withstand several cell culture cycles, spin-coated on a transparent indium thin oxide (ITO) glass. By using this approach, referred to as bio-tSPL (Figure 4), a bone tissue replica with sub-15 nm resolution in x-y and sub-2 nm resolution in z-direction has been patterned over millimeter scale areas, creating unprecedented possibilities for studying how cells interact with the surrounding in the body, and for developing new surfaces that foster cell growth and differentiation for diverse biomedical applications. To this aim, an AFM image bitmap input image of the bone microenvironment is uploaded in the tSPL software, and a series of filtering processes are performed by setting a threshold that increases the number of 0-level pixels (above the threshold) that do not require writing. In this way, the AFM bone input image is divided in two parts: the background (higher topography) and foreground (lower topography) to extract useful topographical information encoded in the pixels. The input image is then patterned on the PMCC resist through the Nanofrazor using a set of parameters optimized to increase throughput and decrease cost. A typical set of parameters includes a pixel size of 16 nm and a pixel dwell-time of 40 μs, operating in pulsed heating mode with a temperature from 1000-1200°C.

Furthermore, the bone tissue replicas fabricated via bio-tSPL can be decorated using *ad hoc* molecules with nanoscale spatial resolution, creating new possibility for reproducing the chemical and physical complexity of biological tissues in the Petry dish. This ability creates the possibility to engineer smart substrates for analytes detection and cell control.

(H2) tSPL for nanomagnetism and magnonics

Tailoring the magnetic properties of materials at the nanoscale plays a fundamental role in the study and design of solid-state spintronic devices, which use the electron spin, in addition to its charge, for data storage and computation. Recently, spin textures (G)[58], have attracted attention as "functional" elements in devices[59-61].

Conventionally, magnetic nanostructures are fabricated via Optical and E-beam lithography, using standard subtractive or additive processes[62]. Other methods are based on locally modifying or damaging the material via ion-irradiation, either by masking or focused beams, for changing the

magnetic properties[16]. Finally, 3D magnetic structures can be fabricated by direct growth via focused electron-beam induced deposition[63] or via two-photon polymerization lithography[64]. However, directly controlling the magnetization orientation deterministically, with nanoscale precision, and in a reversible way is extremely challenging.

Thermally assisted scanning probe lithography (tamSPL)[5] allows to write point-by-point the magnetization orientation, without producing any structural of chemical change, by exploiting a heat-induced purely magnetic phase transition. Tam-SPL is performed on magnetic multilayers characterized by the exchange bias effect[36], such as thin film bilayers composed by a FM in contact with an AF. In such systems, the exchange bias is responsible for pinning the magnetization of the FM in one direction.

The working principle, shown in Figure 7a, is based on performing tSPL while applying an external magnetic field. As the heated probe is displaced across the sample, it locally heats the system above its "blocking temperature", thus temporarily destroying the exchange bias. As the probe is displaced, the previously heated region cools down to room temperature and the exchange bias is re-set in the direction of the applied magnetic field.

By controlling point-by-point the probe temperature, pattern geometry and magnetic field it is possible to write complex spin-textures in a variety of magnetic systems, such as FM/AF bilayers or Synthethic Afs[38] composed by mulprobele FM layers coupled antiferromagnetically with each other.

Importantly, the patterning is fully reversible, and can be erased and rewritten by performing tam-SPL again on the same region. Figure 7b shows a MFM image of patterned magnetic domains. The red (blue) arrow indicates the magnetization direction within (outside) the patterned areas. The spin orientation of the domain walls, i.e., the regions at the domain boundaries where the magnetization rotates, can be controlled precisely by tuning the pattern shape and direction of the external field. In Figure 7c, the black arrows mark the direction of the magnetization point-by-point in the vicinity of the diamond-shaped domain, as calculated via micromagnetic simulations. In addition to magnetic domains and domain walls, by properly designing the magnetic field direction and pattern shape, it is possible to stabilize topologically protected magnetic solitons, such as magnetic vortices and anti-vortices, with highly controlled properties[65].

The precise control of the magnetization opened several possibilities for a variety of applications. Among these, manipulating spin waves using patterned spin textures is an extremely promising

avenue[17]. In fact, spin waves, are being extensively studied as a potential platform for beyond-CMOS computing due to their rich phenomenology, energy efficiency, and nanoscale dimensions[66,67].

Here we review two applications in the field of magnonics, where spin textures patterned via tam-SPL can be employed as waveguides, for confining and steering spin waves in reconfigurable circuits, and as nanoantennas for emitting spin waves.

In the first case[17], shown in Figure 7d, a curved domain wall, is patterned via tam-SPL in a FM/AF bilayer. The magnetization direction on the two sides of the wall is indicated by the red and blue arrows. For exciting spin waves within the domain wall, an oscillating radiofrequency magnetic field was provided by a nanometric metallic antenna, the spin-wave emitter, located in correspondence of the wall. The blue/red color shows simulated propagating spin waves emitted by the antenna, which are confined and guided by the domain wall.

In the second application[68], a curved domain wall patterned in a Synthetic AF is used as a magnonic nanoantenna, for emitting and focusing spin waves. In such system, it is possible to control the shape of the emitted wavefronts, by controlling the shape of the domain wall nanoantenna via tamSPL. Figure 7e shows a simulation and Figure 7f the corresponding experimental time-resolved XMCD image[16] of the spin wave wavefronts, highlighting the focusing effect arising from the concave shape of the wavefronts[68].

In summary, it has been shown that tam-SPL allows to stabilize tailored and reconfigurable spin textures, ranging from 2D domains to 1D domain walls and 0D topological solitons in different magnetic systems among which FM/AF bilayers and synthetic antiferromagnets. This ability creates new possibilities for applications in which the spin texture represents an additional design element for functional spintronic devices. In the field of magnonics, tamSPL spin textures are used as waveguides and basic building blocks for reconfigurable circuits, and as magnonic nanoantennas for emitting shaped spin-wave wavefronts. Further applications are envisioned e.g., regarding the patterning of out-of-plane magnetized materials and three-dimensional spin textures, and the realization of magnon-based computing platforms exploiting the spin-wave interference in continuous films.

(H2) tSPL for nanoelectronics

Graphene oxide (GO) has been patterned by tSPL through the thermochemical interactions and

leads to the formation of reduced graphene oxide (rGO). Both the extent of reduction and the nanoscale regions of rGO have been achieved by tuning the scan speed at several μm/s. The conductivity of rGO is found to be four orders of magnitude higher than that of GO before tSPL patterning. The 100% yield of dozens of rGO ribbons of 12 nm in width (full width at half maximum, FWHM) up to 20 μm on random locations in the GO film has been demonstrated experimentally[9].

In Figure 8, both top-gated and back-gated FETs on 1L MoS_2 as well as graphene have been fabricated through the tSPL technique. Linear I-V curves of the FETs have been observed even at low temperatures as a result of resist residual free, illustrating a low Schottky barrier heights of ~ 0 meV, high on/off ratio of 10, and low subthreshold swing of 64 mV per decade[69].

In a recent work, a high-resolution direct nanocutting of 2D materials have been realized by using the tSPL process. In particular, the nanoscale hot probe induces rapid sublimation or plastic deformation of a polymeric layer, the PPA layer, beneath the 2D materials, resulting the breaking or stretching of the atomic lattice. Various geometries on monolayer $MoTe_2$, MoS_2, and $MoSe_2$ have been successfully demonstrated, including nanoribbons, nanosquares, and other arbitrary test patterns with resolution down to about 20 nm, offering a promising clean, one-step nanopatterning technique for 2D micro/nanoscale devices[70].

Very recently, Riedo et al. utilized the strong interactions between the heated probe and 2D materials to produce atomic defects and hence the p- or n-type doping of the 2D materials. Both the doping extent and polarity can be easily tuned on demand by adjusting the gas environment. As a result, various functional semiconducting devices have been achieved, including the field effect transistors of precise sub-μm spatial control and p-n junctions with a rectification ratio of over 10^4. The doping mechanisms have been investigated by means of X-Ray photoelectron spectroscopy, scanning transmission electron microscopy, and density functional theory. The formation of protruding covalent S-S bonds is responsible for the p-type doping in HCl/ H_2O atmosphere, whereas the S vacancies of MoS_2 is the reason for n-character in N_2 gas[15].

Finally, compact electrochemical metallization cells with excellent electrical performance and reproducible characteristics have been realized by utilizing an ultrasharp 3D metal probe patterned by a thermal nanoscale lithography tool. A well-controlled metallic filament formation has been observed in a highly confined filed at the apex of an atomic scale probe. The ultra-fast switching of 7.5 ns, the write energies of 18 fJ and the set voltages of around 100 mV have been achieved as

a consequence of miniaturization, making them very promising candidates as next-generation volatile and non-volatile memory components[71].

(H1) Reproducibility and data deposition

(H2) Issues with reproducibility

Especially when custom-made AFM are used as tSPL systems, a limited number of patterning conditions (T, load, speed) can be explored in the same experiment, due to the mostly manual procedure and the limitation of the patterning area, corresponding to the maximum x-y piezo extension. This fact limits not only the throughput but also the possibility of making robust reproducibility checks, for example applying just tiny changes in the patterning conditions in order to check materials response in a well-defined environment.

Pattern reproducibility, defined as the fidelity of the pattern to the predefined design, can be affected by the mechanical components of a tSPL. In fact, in both custom-made and commercial tools the probe movement in the x-y-z directions is regulated by piezo actuators, which can exhibit a non-ideal behavior, like thermal drifts, hysteresis, non-linearities, *et cetera*[72]. For example, x-y piezo drifts can lead to deformed shapes, often elongated in one direction, an effect which is more prominent when materials with poor thermal sensitivity are used. In fact, in this case long-term experiments are required to modify the materials and their properties by local heating. The z-piezo drift can in turn affect the temperature at the probe-sample contact and thus thermally activated material transformations.

Other sources of reproducibility issues with tSPL are the materials, the probes and the tSPL setup used.

(H3) Reproducibility issues related to the materials

Materials quality crucially affects the spread of the heat through them and the type and rate of thermochemical reactions. A straightforward example is given by the case of 2D materials. Here, different preparation methods (chemical vapor deposition CVD or mechanical exfoliation) can lead to materials with very different properties (mechanical, electrical, surface chemistry and charge)[73], which may require different patterning conditions to be processed by tSPL. Also, the lack of control on the materials morphology and properties even within the same batch, together with sample contamination (glue and residuals from growth)[74,75] can alter the quality of the thermal

contact, thus affecting the experiment reproducibility, in a way which is difficult to predict and control during tSPL experiments. For polymer samples, new formulations are constantly under development to obtain thermally responsive materials, which undergo fast sublimation or fast chemical reactions upon temperature exposure. Some of them, like PPA are nowadays commercial and their behavior is very reproducible[7,76]. Some other have been used for research purposes and are not commercial[29,33]. In this case, if the polymer power is not optimized and the stoichiometry is not statistically controlled, the thermal response will also be affected in an uncontrollable way. Poor optimizations of polymer resist formulations can limit the film formation itself by spin coating techniques and this will in turn affect the tSPL pattern.

Within the same material, reproducibility issues can also be a consequence of the film thickness. For example, the number of layers in 2D materials can affect the heat spreading. This makes the response of one layer material very different from that of a few layers or bulk material[77,78]. Finally, as the thermal properties of the substrate also affect the heat spreading, it is recommended to use the same substrate for deposition to make experiments reproducible, especially when very thin films are used and the heat spreading to the substrate is more prominent.

(H3) Reproducibility related to the probe

The tSPL probes generally undergo variations during scans performed at high temperature and in contact with the surface. In particular, the probe size can be affected by wear forces (probe blunting) and accumulation of materials at its surface (probe contamination). The probe size can be controlled in situ by checking that the adhesion force or the adhesion length in single force curves is not varying during the experiments. Both parameters in fact, increase as probe size increases and the increased probe size also affects the load applied to the sample, finally impacting on the pattern resolution. Material accumulation at the probe surface can also change (increase) the electrical resistance, thus affecting the probe temperature. Dopants migration from the cantilever arms to the heater region due to high temperature scans is a common form of cantilever aging, that will affect in the opposite way the heater electrical resistance, making it lower[1]. This fact makes the temperature associated to the externally applied voltage lower over repeated scans. Due to the above-mentioned probe variations over time, temperature calibrations need to be often repeated during tSPL experiments to check that the patterning parameters are maintained according to the design. Another parameter which is typically not predictable in tSPL is the amount

and the sign (positive or negative) of the cantilever deflection occurring in consequence of the temperature increase (thermally induced cantilever bending)[19]. This parameter in turn affects the effective load during patterning.

(H3) Reproducibility related to the tSPL setup

Finally, another factor that can affect the reproducibility of measurements is the actual tSPL system used. As mentioned before, tSPL can be performed with custom-made and commercial setups. The two systems have different electromechanical components and use different cantilevers. Also, the patterning parameters are differently defined. In custom-made setups the patterning time, expressed in seconds·μm^{-1}, is the inverse of the scanning speed, i.e., it is the time required to scan a single line divided by the physical size of that line. The patterning load is obtained from the cantilever deflection, expressed in nm after sensitivity calculations, mulprobelied by the cantilever spring constant, as customary in contact-mode based AFM force measurements[79]. In commercial setups the hot probe touches discrete positions of the surface to be patterned, thus the patterning time depends on the dwell time (heating time) and the patterning step size **(G)**, both set independently. The load is set by the capacitive bending of the cantilever, once contact with the surface is established[80]. In the absence of a unique parameter identification, in order to standardize measurement conditions or compare results from different laboratories/countries, the best practice would be to tune different patterning conditions and consider as equivalent those conditions that produce the same transformation in a reference material. This transformation, being it physical or chemical, will in turn be quantified through independent measurements/techniques, like AFM topography, Kelvin Probe force microscopy, current sensing AFM, Raman spectroscopy, fluorescence microscopy, *et cetera*.

Variables affecting tSPL reproducibility		Effect on the outcome	Mitigation strategies
Environment	Ambient humidity (thermal tSPL) Ambient humidity and chemistry (gas flow rate, gas concentration, chamber pre-conditioning) (thermochemical tSPL)	No reaction occurring/low reaction yield (high ambient humidity, low gas flow rates and low concentration). Etching/damage (high gas flow rates and high gas concentration)	Process control (materials, environment, gases and gas flow conditions) (see Refs 7, 8)
	Air exposure after tSPL patterning	Surface passivation and changes over time	For device applications, coating the surface with an inert layer immediately after patterning can improve pattern durability (see Ref 19)

Patterning conditions	Load (setpoint/writing height) Speed: - Scan rate, number of lines, scan size (custom-made setups) - Dwell time, pixel number, step size (commercial tSPL) Heater temperature	No reaction occurring/low reaction yield (low load/temperature, high speed). Risk of sample damage (high load/temperature, low speed) Different chemical reactions in function of the heater temperature	The patterning parameters can be tailored with high level of accuracy in order to obtain the desired transformation reproducibly, depending on the used material (see Refs 7,8)
Hardware	Vibrations Drifts, piezo non-idealities	Non-homogeneous thermal contact Distorted features	Closed loop technology Commercial tSPL designs feature high precision movements and cantilever positioning
Sample and Substrate	Substrate cleaning/pretreatments Sample cleanliness/residuals Sample preparation technique	Affect tSPL resist deposition (spin coating) Affect tSPL resist deposition (spin coating). No reaction occurring/low reaction yield Yield of thermochemical rections/thermal response of the material	Substrate cleaning protocols guarantee good quality of the spin coated resist film (see Ref 19) Process/materials control Slight differences could exist among materials purchased from different providers (see Ref 8)
Lithographic process (lift-off)	Etching time after patterning (TMAH 31hemica) Lift-off time (remover PG)	Sample damage and features enlargement Complete removal of metal contacts, especially with thin metal films	Control of etching time is critical with TMHA (about 2s/nm) (see Ref 19) Using thick sacrificial layers (PMGI, about 200 nm) and thick metal films (≥ 20 nm) helps hold of metal contacts (see Ref 19)
tSPL resist	Polymer formula/stoichiometry	Affects polymer film formation (spin coating) and the occurrence/temperature of thermochemical reactions	Process control, especially with non-commercial polymer films (see Ref 7)
Set-up	Commercial tSPL uses probes with lower runaway temperature Customized tSPL use probes with higher runaway temperature	No reaction occurring/lower reaction yields in commercial setups using the same resist	In the absence of the possibility to opt for different cantilevers, using a substrate with poor thermal conductivity help limiting the heat spreading towards the substrate

Table 1. Variables influencing the tSPL reproducibility, effect on the outcome and mitigation strategies

(H2) Data deposition

No standards for data deposition, data format and specific repositories exist to date for tSPL. Nevertheless, it must be considered that the size of images that can be produced during tSPL experiments and after patterning to verify functional transformations have the size of standard

AFM images (few tens of MB). Also, the volume of images is limited compared to other imaging techniques[81,82]. Raw and processed (.tiff,.jpg,.bmp) images can thus be easily stored and shared using open access available and academic repositories (OneDrive, Dropbox, WeTransfer). Commercial tSPL systems usually output several graphs, like IV, T vs dissipated power, T vs V curves etc. that can be exported in .cvs and.txt formats. Additionally, in the same commercial tSPL setups the patterning conditions are automatically saved in html format. For custom made setups, patterning conditions can be recorded using dedicated scripts (Matlab, Python) that can be made available in open platforms for data sharing. Open software for AFM data processing, like Gwyddion and WSxM can be used for processing the images obtained before, during and after patterning, in addition to the processing software of the actual system used. All these features facilitate the development of common field standards.

To make easier the data processing and comparisons among different experiments and laboratories, it would be desirable to have common rules for the definition of the patterning parameters in a univocal way. For example, the probe temperature is often difficult to quantify, as it is affected by the heat transport through both the probe and the sample. In this case, the heater temperature can be a more convenient parameter, as it comes from a direct measurement. The probe size and load can be tracked through the adhesion force and total cantilever deflection measurements respectively, as detailed in the Reproducibility session. Finally, keeping a copy of the raw, unprocessed data in operational units, typically in Volts, together with calibrations factors and cantilever characteristics (ex, optical sensitivity, spring constant, thermal runaway) may facilitate the processing to other operators/research groups according to their specific needs and for results comparison.

Output data	Output format	Output size (range)	Repository
Patterning and imaging conditions (temperature, speed load, resolution), calibration data	All recorded automatically during the experiment. They can be exported as .txt files (commercial tSPL) Manual recording or through scripts (Matlab) integrated in the AFM software (custom-made tSPL) (Refs 12, 22)	Few KB	All data types can be saved, made available and shared using academic repositories (Onedrive, Dropbox, WeTransfer etc)
Images collected before, during and after patterning	Data format depends on the tSPL system used Raw data are processable with free AFM processing softwares and can be be exported as image files (.jpg, .bmp, .tiff)	< 1MB/image channel	

Curves: F vs z, R vs V (customized AFM) I vs V, T vs V, P vs T, I vs z (commercial tSPL)	Raw data format depends on the used system Both exportable as .cvs, .txt files	Few KB/curve	

Table 2. Output and data format

Minimum reporting standards should include the patterning conditions (temperature, patterning speed, load and resolution) and relevant images of the process under study, showing the pattern features/characteristic size and the change in material properties after patterning. A minimum of 256x256 pixel images should be collected to guarantee good image quality, as it is customary in scanning probe microscopy.

(H1) Limitations and optimization

(H2) Resolution limitations

The tSPL method can produce patterning lines with lateral size below 10 nm and depth of 1 nm. The extremely high lateral resolution is limited by the probe size and shape. Resolution is also limited by the size and quality of the thermal contact, that depend on the load and the time the probe is in contact with each point of the surface while patterning. These parameters can be adjusted and vary depending on the setup used (dwell time or pixel time **(G)**, for example, define the probe-sample contact time in commercial tSPL setups, while the same contact time is determined by the scanning rate in customized setups). Other factors limiting the resolution are the film thickness and the actual patterning temperature. In tSPL, the ultimate width resolution has been obtained using very thin films of highly thermal sensitive materials, where the amount of material to be evaporated/converted is small, allowing for the application of small *dwell times* and low temperatures, thus limiting the lateral spreading of the heat. Features with 8 nm half pitch have been obtained using polymeric films with thickness of less than 10 nm[16,29,83,84].

(H2) Speed limitations

In tSPL the patterning speed is limited by the setup used, in particular by the actuation frequency of the mechanical components of the system and the trade-off between scan speed and positional accuracy[80]. A limiting factor for the speed is also given by the thermal properties of the materials under processing, like the sublimation T, the activation energy for chemical conversion, the

thermal diffusion. Practical throughput of 1 mm/s scan speed at 100 kHz pixel rate are normally achieved with polymeric resists[3,31], while poorly responsive materials, like MoS_2 required scanning speeds hundreds of times lower[15].

(H2) 3D patterning limitations

Patterning very deep features means removing or chemically converting a relatively high amount of material, thus it requires thick films and high applied temperature and pressure. It has to be noticed that the conditions of high temperature and load necessary to achieve 3D patterning are incompatible with the conditions to achieve high lateral resolution, thus deep patterns will be obtained at the expenses of larger feature size[2,54,85]. The depth of the achievable features in tSPL is also limited by the height of the probe cone (typical values ~ 500 nm)[80].

(H2) Throughput limitations

Throughput is limited by the scanning speed and by the physical size of the final pattern. It can be improved by parallelization, using mulprobele heatable cantilevers working in parallel, and by using different processes, ex. Laser heating (faster, scan speed: 5 mm/s) for low resolution features (bigger than 600 nm) and thermal cantilevers (slower, scan speed: 1 mm/s) for high resolution features in the nanometer range. The laser writer module has already been integrated in commercial setups for wafer size patterning (10x10 cm^2). In commercial tSPL setups the multi probe extension module is currently under development.

(H2) Customized components

In custom made designs, limitations arise from the fact that specific components of standard AFM systems need to be replaced with custom components for tSPL experiments to be performed. For example, special cantilever holders have been designed which consist in printed circuit boards (PCB) with metallic pads that allow for the electrical connection. These cantilever holders may interfere with the laser optical path, affecting the easiness of the laser alignment. Limitations in the shape and number of the patterned areas are also present with custom made tSPL setups. Single lines and shapes, like squares and rectangles, can be drawn without issues. Nevertheless, dedicated scripts are needed to increase the flexibility of the setup in writing arbitrary shapes and reproducing them repeatedly within the maximum x-y piezo extension (that for most AFM is ≤ 100 mm) and

beyond the maximum allowed AFM imaging size. These limitations are by far overcome in commercial setups.

(H2) Piezo non idealities

Even if current setups are highly optimized and integrate closed loop technology for scanners positioning, piezo drifts (**G**), a common source of artifacts in AFM imaging[72], can also limit the performances of tSPL setups. Drifts of the voltage applied to the heater or stage vibrations can also occasionally occur affecting the probe-sample contact temperature and the patterning results.

(H2) Probe availability

As for now, few types of cantilevers are available for tSPL, which are custom made or commercial[1,3,86]. Depending on the probe used, probe radius ranges from 2-10 nm, the spring constant from 0.9-1.5 N/m, while the maximum heater temperature ranges from 800-1100°C. Depending on the specific application, a wider range of probe sizes and cantilever spring constant may be required, which are not currently available.

(H2) Environment of thermochemical reactions

Commercial setups only allow for experiments in inert environment (N_2, Ar) or in ambient conditions. This fact limits the versatility of the equipment, as some reactions need specific environments to occur. In turn, reactive gases may damage and oxidize metallic parts and delicate components of the tSPL setups. Custom made AFM are more versatile, and they have been integrated with a liquid cell that allow for the flow of small volumes of reactive gases, like HCl and water vapors[15]. Though small volumes and low gas concentration are used, periodic cleaning procedures are in this case necessary for a good maintenance of the system and to avoid frequent components replacements.

(H2) Unexpected outcomes

Finally unexpected outcomes can arise from non-optimized protocols for sample preparation, changes in the probe properties and hardware instabilities (vibrations, drifts) during patterning. Environmental conditions (i.e., the relative humidity) must be controlled and can also generate

unexpected outcomes[29]. Unexpected results related to the samples to be processed can only be limited by an accurate knowledge on the sample characteristics *a priori* before tSPL experiments and a good control on the sample preparation method. The constancy of the probe characteristics can be rapidly checked *in situ* during tSPL experiments through calibrations, thus this is less critical.

(H1) Outlook

Future developments of tSPL rely on the specific needs and associated technical challenges related to the different fields of application. Using tSPL for producing highly localized tunable physical and chemical transformations is a powerful strategy that we just started to explore, and which is attracting considerable attention in the community. In this framework, however, some limitations such as low interface temperature and probe wear limit the wide applicability of tSPL. Developing enhanced thermal probes as well as adapting the technique to the specific applications, represent an important ongoing effort and will allow to truly advance the universality of the technique in the desired field. Below here we discuss challenges, novel approaches, and priorities that must be considered in the next 5-10 years to fully realize the promise of tSPL in biomedicine, nanomegnetism and nanolectronics.

For tissue engineering applications, it is required to pattern large areas that are meaningful for cell culture studies and for use of tSPL-fabricated surfaces in promoting tissue regeneration in human patients. Indeed, human cells range from μm to mm in size when attached to a surface, meaning that in order to conduct biological studies it would be optimal to pattern biologically relevant structures and motifs in the cm^2 range. Reproducing the complexity of biological tissues with nanoscale precision over cm^2 areas using tSPL requires an unreasonable long time and an extremely large number of expensive thermal probes. Furthermore, tSPL has a high potential for patterning surfaces of medical devices to improve tissue regeneration, histocompatibility, and to reduce complications such as adverse reactions leading to implant rejection. However, these applications require even larger areas, and the possibility to either transfer the pattern on implants and other medical devices or to directly relocate the patterned polymer film directly on the device surface is of paramount importance for these applications. To increase the throughput, in addition to the strategies described here in paragraph 2.5, there are some future improvements that can be considered. First, the possibility to parallelize the patterning by means of an array of tSPL probes

would immediately increase the throughput. Initially, linear arrays of up to ten probes could be developed, where each probe can be used in series. This approach will not allow to write in parallel, but it will save time in probe-exchange, decreasing the overall time required to pattern a large area. A more complex and effective solution would require each probe to write in parallel. This option could be first achieved with a small number of probes to reduce complexity, since even only three probes could decrease the patterning time of one month in only ten days. Another approach to increase throughput is to find strategies to reduce contamination of the thermal probe during patterning, such as for example using a laminar flow of inert gases in the NanoFrazor chamber and/or adding an *in-situ* probe flash annealing step via probe baking or mechanical scratching. Reducing probe contamination not only increases the throughput but also dramatically decreases the cost of large-scale patterning.

Another limitation of tSPL for biomedicine-oriented applications is the limited depth which can be patterned in a substrate. This limitation is mainly due to the small size and shape of the probe/cantilever system. To overcome this problem, one possibility is to amplify the pattern depth by transfer the pattern into the underlying substrate through different etching steps. Another possibility is to develop a thermal probe with *ad hoc* size and shape that can allow deeper indents. Finally, using laser writing combined with tSPL could obviate to this issue.

Regarding applications of tSPL in nanomagnetism and spintronics, the investigation so far focused primarily on ferromagnetic thin film materials, which historically have driven the development of the field. The rapid rise of Wan-der-Waals magnets[87], i.e., materials which maintain or develop magnetic properties down to the monolayer limit, represents one of the most promising recent development of the field. They combine the added functionality deriving from spintronics, with the vast phenomenology of 2D materials, opening the way to novel devices and functionalities exploiting exotic effects. Recently, magnetic materials characterized by other types of magnetic ordering, such as ferromagnets or antiferromagnets[88], have raised the attention of the community due to their unique properties which makes them markedly distinct from ferromagnets. Advances of tSPL in the field of nanomagnetism and spintronics will be strongly based on developing and improving the technology, as well as on investigating novel advanced magnetic materials. The combination of these two aspects represents an extremely promising avenue for future developments in the next years.

Regarding nanoelectronics applications, in addition to throughput, an improvement in lateral resolution below 10 nm would be greatly beneficial for the performances of the next generation electronic devices. Another important aspect for these applications is the reproducibility and robustness of the fabrication process.

Glossary terms:

Blocking temperature: Temperature above which the exchange bias effect vanishes.

Cantilever deflection: Bending of the cantilever on the surface. It is measured using an optical lever method where a laser beam, reflected from the upper surface of the cantilever, measures the cantilever angle at the position of the reflection. For thermal cantilever, the deflection is measured by monitoring the heat exchange between the cantilever's read heater and the substrate: a constant voltage is applied to the heater via a series resistance and the current flowing through the heater is measured. The reader signal is converted into depth using the Piezo calibration process.

Closed loop lithography: In commercial tSPL, after one patterning line the topography of the written line is imaged with the cold probe. A feedback algorithm adjusts the patterning conditions to make the pattern as close as possible to the design.

Deprotection reaction: The process of removing a protecting group that is present in a polymer resist to expose specific chemical groups at the surface of the resist film.

Drift: unwanted motion of the actuators that control the sample position relative to the probe in the three directions. It can depend on temperature fluctuations or on piezo non-idealities. It affects the probe-sample contact (z-drift) or it can give rise to distorted features (x-y drift).

Dwell time/heating time: In commercial tSPL setups, this is the time (in ms) that the heated cantilever spends in each position (pixel) of the pattern.

Exchange bias: Effect occurring at the interface between a ferromagnetic and an antiferromagnetic material, which causes the shift in the hysteresis loop of the ferromagnet, i.e. the "pinning" of the magnetization of the ferromagnet in one direction.

Joule heating: Generation of heat associated to the flow of an electric current in a resistive material. It is exploited in thermal probes for raising the probe temperature.

Magnetization dynamics: Time-dependent evolution of the magnetization in magnetic materials.

Marker-less patterning: Patterning technique that does not require alignment markers. Alignment markers are used in techniques like the electron beam lithography as references for the

correct positioning of the pattern within the sample surface. This is because the patterning areas cannot be reached with an electron beam without destroying at the same time the resist to be patterned.

Mask-less patterning: Patterning technique that does not require a physical mask to protect the areas of the samples from unwanted transformations. This is different from optical lithography, where usually a mask is used to protect the area of the sample from light irradiation.

Oxidation sharpening: Process widely used for sharpening AFM probes, i.e., for reducing their radius of curvature. It consists of a thermal oxidation step followed by the removal of the oxide.

Patterning step size: In commercial tSPL setups, this is the number of subsequent indentation points in a line.

Pixel time: In commercial tSPL setups, it indicates the scanning rate and more precisely, the time interval between adjacent probe indentations

Pixel size: In commercial tSPL, it corresponds to the distance between two adjacent writing pixels.

Plasma dry etching: Removal of plastic or other semiconductor material using plasma as opposed to chemical treatment. The excited ions in the plasma collide with the material and remove it without any chemicals.

Schottky Barriers: An electrostatic depletion layer formed at the junction of a metal and a semiconductor, which causes it to act as an electrical rectifier.

Spin textures: Non-uniform configurations of the magnetization in magnetic materials, such as domain walls, magnetic vortices or magnetic skyrmions.

Spin waves (or magnons): Wave-like perturbations in the orientation of the magnetization, which propagate in magnetic materials.

Spring constant: The force needed to stretch or press a spring, divided by the distance that the spring gets longer or shorter. The force F that a spring exerts on the object is defined by the Hooke's law as: $F = -kx$ where the proportional constant k is called the spring constant and x is the displacement.

Probe load: The force applied by the probe on the sample during pattern.

Thermal bending: A bimorph effect of thermal cantilever, which goes approximately linear with temperature. For tSPL patterning it is obtained by modulating the force voltages between the sample and the thermal cantilever and performing a series of electrostatically actuated approach experiments at different initial cantilever heights and writer temperatures.

Total cantilever deflection: The sum of the patterning setpoint, which is a feedback loop that is used to adjusts the height of the cantilever to keep the deflection signal at a constant value, plus the cantilever thermal bending at the patterning temperature (refer to “cantilever bending” and “thermal bending”).

Figures

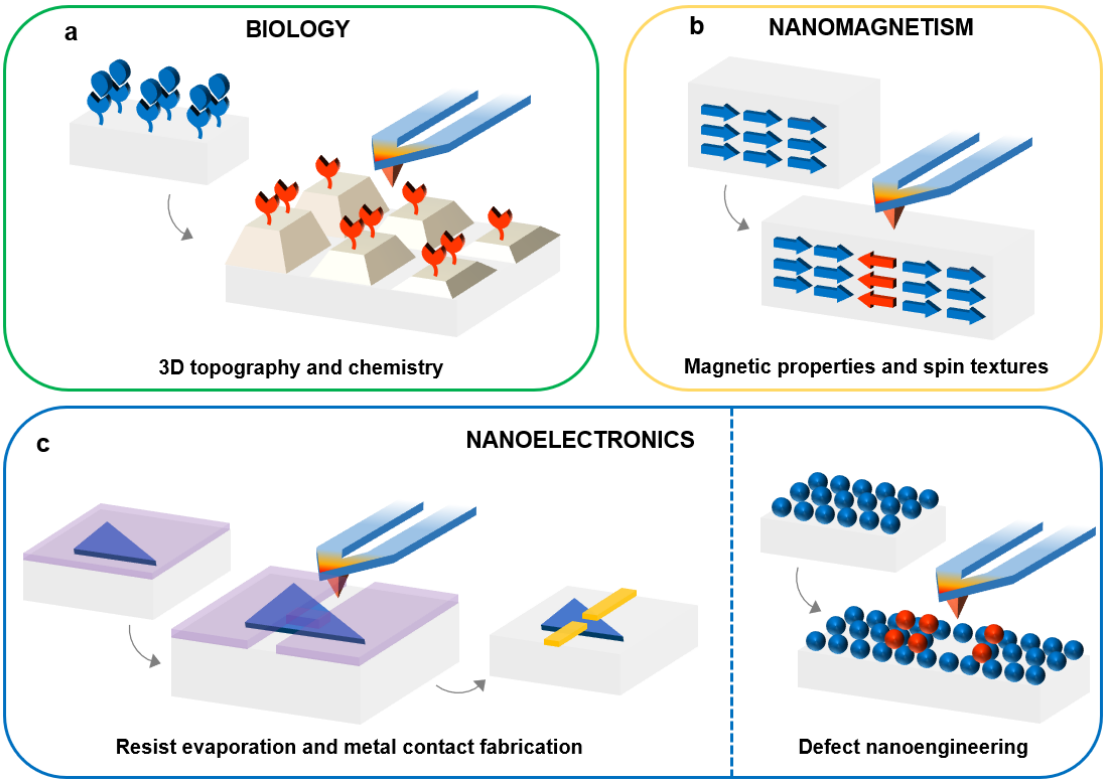

Figure 1. a. Patterning chemical gradients for biology. tSPL is used for tunably deprotecting functional groups with nanoscale resolution. Chemical and protein gradients can be created by precisely controlling the concentration of the reactive groups and subsequently functionalizing the surface. **B.** Patterning magnetic materials. Thermally assisted magnetic scanning probe lithography (tam-SPL) is used for stabilizing spin textures such as magnetic domains and domain walls in ferromagnetic materials. **C.** tSPL for nanoelectronics. Left: patterning metal contacts on 2D materials. Local sublimation of a molecular resist via tSPL is employed for fabricating high performance metal contacts on 2D materials for nanoelectronics. Right: defect nanoengineering for nanoelectronics. tSPL is used for locally creating defects in the crystalline structure of 2D materials, allowing to tune their transport properties.

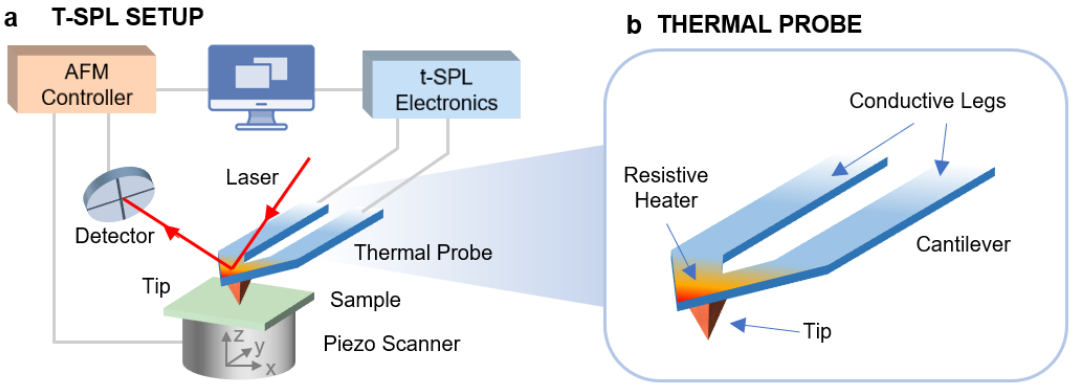

Figure 2. a. Schematic of the "standard" tSPL setup using a customized Atomic Force Microscope (AFM). The AFM scanners and feedback system allow to sweep the heated probe in contact with the sample. While scanning, the temperature of the probe is controlled by the tSPL electronics. **b.** Schematic of a thermal probe, consisting of a U-shaped cantilever with two conductive legs, and a resistive heater located above the nanometric probe.

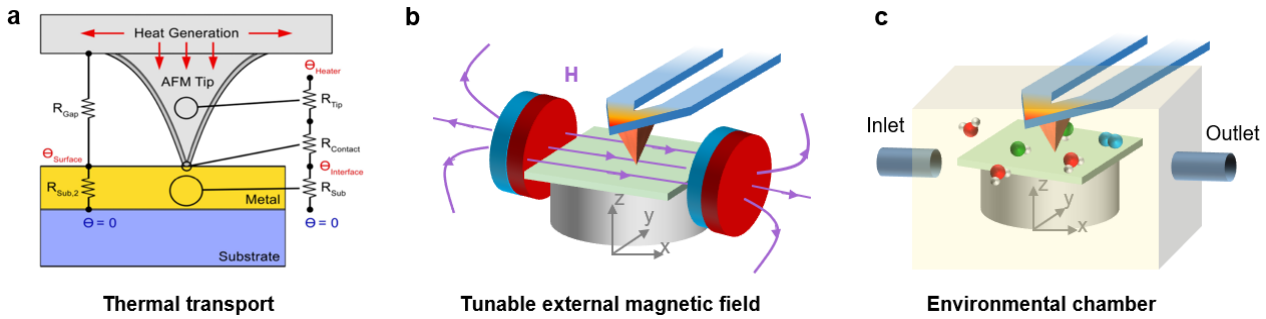

Figure 3. a. Schematic of the heat conduction circuit from a tSPL thermal probe to the substrate. Heat is generated above the probe, and diffuses towards the substrate. The thermal resistances (R) and temperatures (Q) are indicated for each element. **b.** Schematic for magnetic applications: an external magnetic field is applied while performing tSPL. **c.** Schematic of tSPL including an environmental chamber used for applications ranging from biology and nanoelectronics.

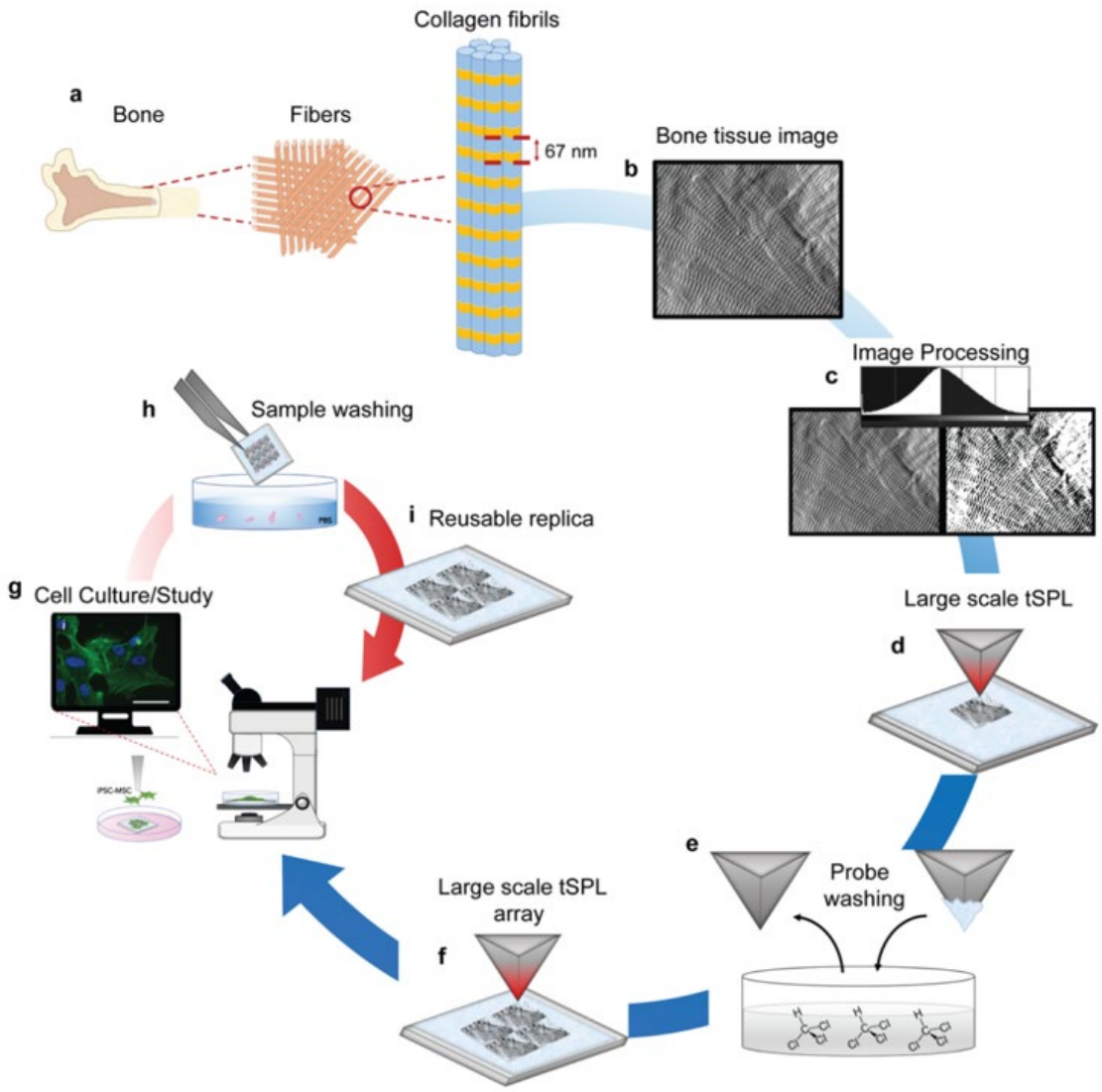

Figure 4. Schematic representation of Bio-tSPL to produce mm size bone tissue replicas. (a) Architecture of bone tissue composed of twisted plywood arranged fibers containing collagen fibrils with the characteristic 67 nm periodicity. **(b)** AFM amplitude image of the bone tissue. **(c)** Threshold filtering of the bone image to increase throughput. **(d)** Patterning of large-scale bone replicas in the PMCC resist using the filtered input image in **(c)** and optimized writing parameters. **(e)** Cleaning of the soiled thermal probe with chloroform. **(f)** Further patterning of large-scale bone replicas in the PMCC resist. **(g)** Cell culture on the mm-sized bone replicas. **(h)** Cell removal and sample washing. **(i)** Reuse of the mm-sized bone replicas for mulprobele cell culture studies.

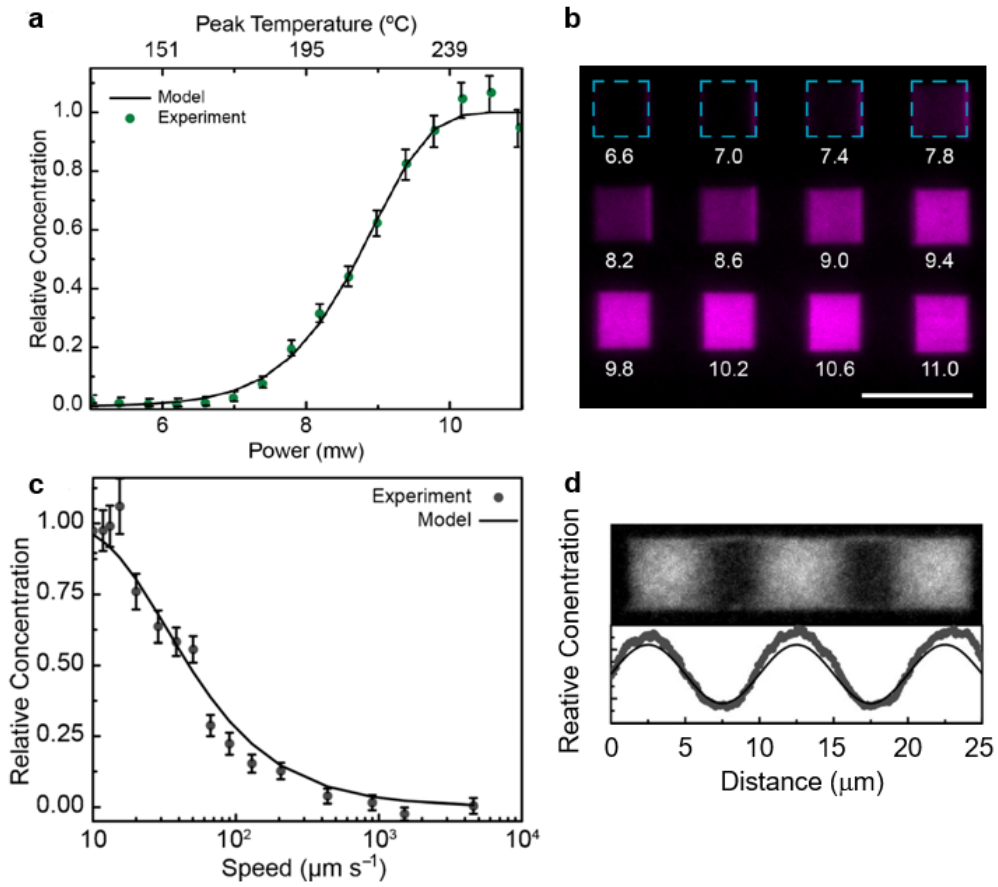

Figure 5. e. Effect of the patterning temperature on the reaction output. By controlling the temperature, the relative concentration of reactive amine groups on a PMCC polymer surface can be controlled precisely. **b.** Fluorescence image showing square areas of thermally deprotected amine groups labeled with NHS dye, patterned at different heating powers, in the range 6.6-11.0 mW. Scale bar: 10 mm **c.** Effect of the patterning speed on the reaction output. The output concentration is increased by reducing the patterning speed. **d.** Fluorescence intensity of a sinusoidal pattern realized by varying the patterning speed at fixed temperature.

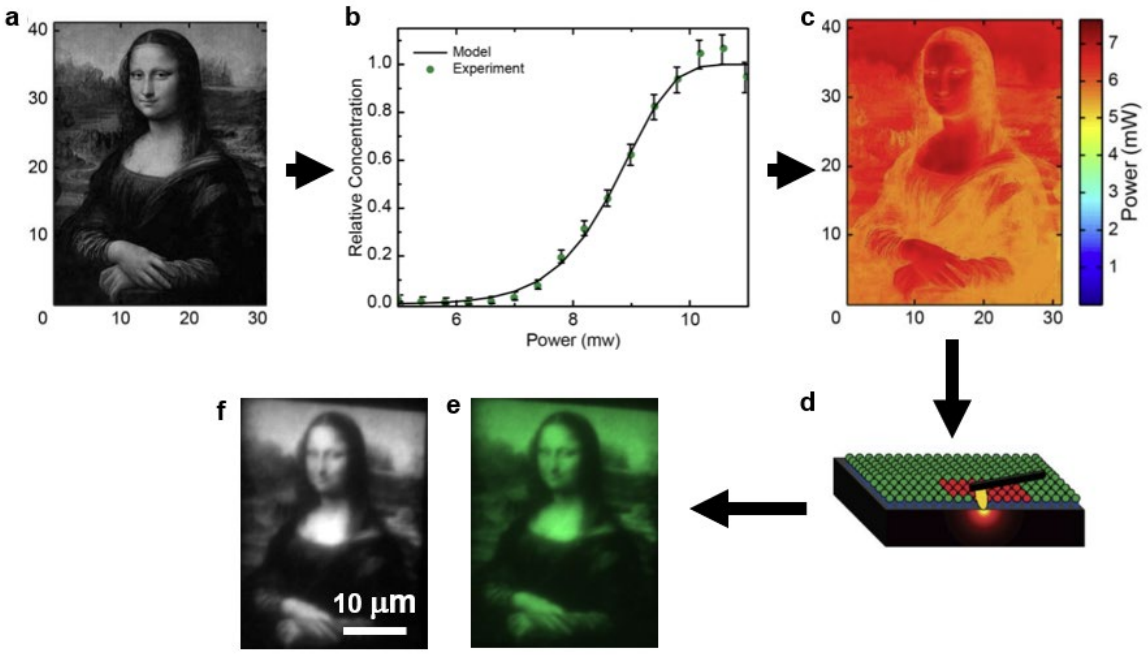

Figure 6. Workflow for the generation of chemical gradients. **a**. User defined greyscale image. **b.** Calibration of relative concentration vs. heater power/temperature. **c.** Generation of power map based on (b). **d.** tSPL fabrication. **e, f.** Chemical gradient images, **e** being the AFM topography and **f** the fluorescence image after dye immobilization on the pattern.

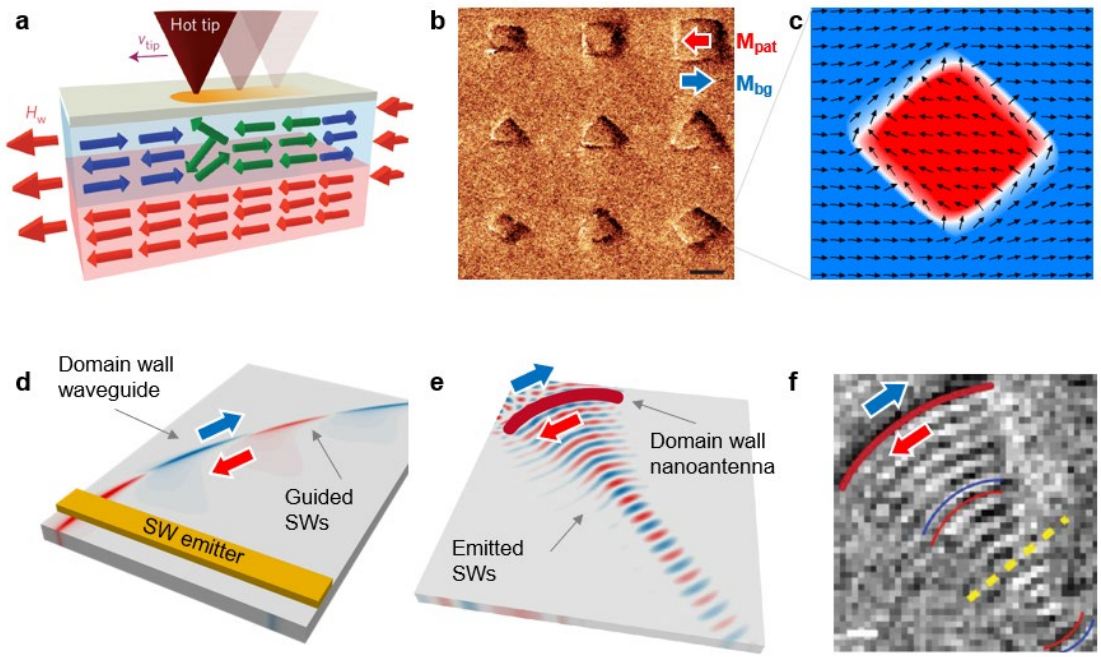

Figure 7. a. Schematic of thermally assisted magnetic scanning probe lithography (tam-SPL). Spin textures are stabilized by sweeping the heated probe in presence of an external magnetic field. **b.** Patterned magnetic domains imaged via magnetic force microscopy. The arrows indicate the direction of the magnetization in the pattern (M_{pat}) and outside (M_{bg}). Scale bar 2 mm. **c.** Micromagnetic simulations showing the magnetization (black arrows) of the diamond-shaped magnetic domain in **b**. **d.** Schematic of a domain wall-based waveguide for spin waves. Spin waves are emitted by the antenna (yellow) and propagate within the domain wall. **e.** Schematic of a domain wall-based nanoantenna for spin waves. The domain wall, set in oscillation, emits shaped spin wave wavefronts. **f.** Experimental X-Ray Microscopy snapshot showing curved spin wave wavefronts emitted by the domain wall (thick red line). Scale bar: 500 nm.

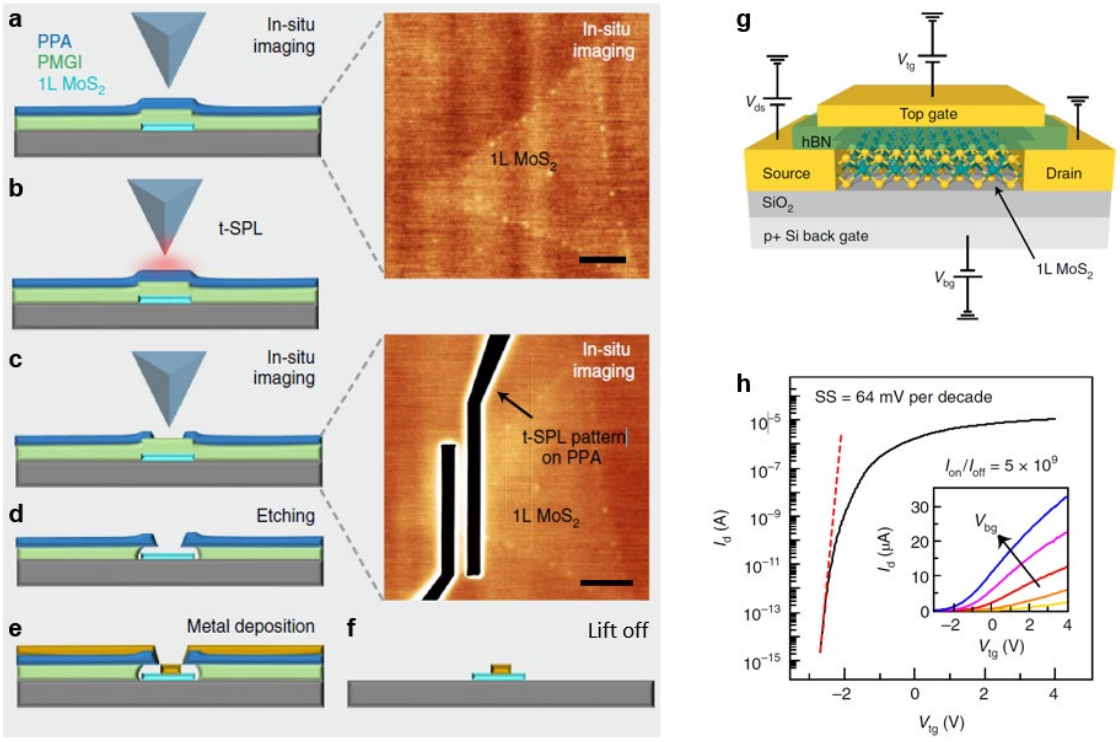

Figure 8. a-f. Schematic of the electrodes fabrication process via tSPL, including the spin coating of two polymer stack on a monolayer flake (**a**), tSPL patterning of the top thermal resist (**b-c**), wet etching of the sacrificing resist (**d**), metal deposition (**e**) and lift-off process (**f**). Insets: The *in-situ* identification of the monolayer MoS_2 flake (0.65 nm) under the thick polymer stack (230 nm) and the subsequent tSPL patterning of the thermal resist, without the need of markers and masks. **g.** Schematic cross-section and electrical connections of a top-gate FET. Both the source–drain contacts and the aligned top-gate are patterned via tSPL. The structure comprises the degenerately doped Si substrate as global back gate, a 285 nm thermal SiO_2 as back-gate dielectric, and a 15 nm h-BN layer as top-gate dielectric. **h.** Room-temperature transfer curve of the top-gate FET measured at V_{ds}=2 V. Subthreshold swing (SS)=64 mV per decade, I_{on}/I_{off}=5×10^9. In the inset, transfer curves at different back-gate voltages ranging from V_{bg}=−20 V (yellow curve) to V_{bg}=20 V (blue curve).

References:

1 Garcia, R., Knoll, A. W. & Riedo, E. Advanced scanning probe lithography. *Nat Nanotechnol* **9**, 577-587, doi:10.1038/Nnano.2014.157 (2014).

2 Pires, D. *et al.* Nanoscale Three-Dimensional Patterning of Molecular Resists by Scanning Probes. *Science* **328**, 732-735, doi:10.1126/science.1187851 (2010).

3 Szoszkiewicz, R. *et al.* High-speed, sub-15 nm feature size thermochemical nanolithography. *Nano letters* **7**, 1064-1069 (2007).

4 Rawlings, C. *et al.* Accurate Location and Manipulation of Nanoscaled Objects Buried under Spin-Coated Films. *ACS Nano* **9**, 6188-6195, doi:10.1021/acsnano.5b01485 (2015).

5 Albisetti, E. *et al.* Nanopatterning reconfigurable magnetic landscapes via thermally assisted scanning probe lithography. *Nature Nanotechnology* **11**, 545-551, doi:10.1038/nnano.2016.25 (2016).

6 Wang, D. B. *et al.* Thermochemical Nanolithography of Multifunctional a Nanotemplates for Assembling Nano-objects. *Adv Funct Mater* **19**, 3696-3702, doi:10.1002/adfm.200901057 (2009).

7 Knoll, A. W. *et al.* Probe-based 3-D nanolithography using self-amplified depolymerization polymers. *Adv Mater* **22**, 3361-3365, doi:10.1002/adma.200904386 (2010).

8 Coulembier, O. *et al.* Probe-Based Nanolithography: Self-Amplified Depolymerization Media for Dry Lithography. *Macromolecules* **43**, 572-574, doi:10.1021/ma9019152 (2010).

9 Wei, Z. *et al.* Nanoscale tunable reduction of graphene oxide for graphene electronics. *Science* **328**, 1373-1376 (2010).

10 Liu, X. Y. *et al.* High-throughput protein nanopatterning. *Faraday Discuss* **219**, 33-43, doi:10.1039/c9fd00025a (2019).

11 Kim, S. *et al.* Direct fabrication of arbitrary-shaped ferroelectric nanostructures on plastic, glass, and silicon substrates. *Adv Mater* **23**, 3786-3790, doi:10.1002/adma.201101991 (2011).

12 King, W. P. *et al.* Heated atomic force microscope cantilevers and their applications. *Annual Review of Heat Transfer* **16** (2013).

13 Xiangyu Liu, A. Z., Martina Sladkova-Faure, Liyuan Xie, Marcus Weck, Xiaorui Zheng, Elisa Riedo, and Giuseppe Maria de Peppo. Cost and Time Effective Lithography of Reusable Millimeter Size Bone Tissue Replicas With Sub-10nm Feature Size on A Biocompatible Polymer. *Advance Functional Materials* **https://doi.org/10.1002/adfm.202008662**, doi:https://doi.org/10.1002/adfm.202008662 (2021).

14 Liu, X. *et al.* Sub-10 nm Resolution Patterning of Pockets for Enzyme Immobilization with Independent Density and Quasi-3D Topography Control. *ACS Appl Mater Interfaces* **11**, 41780-41790, doi:10.1021/acsami.9b11844 (2019).

15 Zheng, X. *et al.* Spatial defects nanoengineering for bipolar conductivity in MoS2. *Nat Commun* **11**, 3463, doi:10.1038/s41467-020-17241-1 (2020).

16 Zheng, X. R. *et al.* Patterning metal contacts on monolayer MoS2 with vanishing Schottky barriers using thermal nanolithography. *Nat Electron* **2**, 17-25, doi:10.1038/s41928-018-0191-0 (2019).

17 Albisetti, E. *et al.* Nanoscale spin-wave circuits based on engineered reconfigurable spin-textures. *Communications Physics* **1**, 56, doi:10.1038/s42005-018-0056-x (2018).

18 Mamin, H. & Rugar, D. Thermomechanical writing with an atomic force microscope probe. *Applied Physics Letters* **61**, 1003-1005 (1992).

19 Lee, J. *et al.* Electrical, thermal, and mechanical characterization of silicon microcantilever heaters. *Journal of Microelectromechanical Systems* **15**, 1644-1655 (2006).
20 Chui, B. W. *et al.* Low-stiffness silicon cantilevers with integrated heaters and piezoresistive sensors for high-density AFM thermomechanical data storage. *Journal of Microelectromechanical Systems* **7**, 69-78 (1998).
21 King, W. P. *et al.* Design of atomic force microscope cantilevers for combined thermomechanical writing and thermal reading in array operation. *Journal of Microelectromechanical Systems* **11**, 765-774 (2002).
22 Rawlings, C. *et al.* Accurate location and manipulation of nanoscaled objects buried under spin-coated films. *ACS nano* **9**, 6188-6195 (2015).
23 Paul, P., Knoll, A., Holzner, F. & Duerig, U. Field stitching in thermal probe lithography by means of surface roughness correlation. *Nanotechnology* **23**, 385307 (2012).
24 Rawlings, C., Duerig, U., Hedrick, J., Coady, D. & Knoll, A. W. Nanometer accurate markerless pattern overlay using thermal scanning probe lithography. *IEEE Transactions on Nanotechnology* **13**, 1204-1212 (2014).
25 Fletcher, P. C. *et al.* Wear-resistant diamond nanoprobe probes with integrated silicon heater for probe-based nanomanufacturing. *ACS nano* **4**, 3338-3344 (2010).
26 Spieser, M., Rawlings, C., Lörtscher, E., Duerig, U. & Knoll, A. Comprehensive modeling of Joule heated cantilever probes. *Journal of applied physics* **121**, 174503 (2017).
27 Gotsmann, B. & Lantz, M. Quantized thermal transport across contacts of rough surfaces. *Nature materials* **12**, 59-65 (2013).
28 Heinz, W. F. & Hoh, J. H. Spatially resolved force spectroscopy of biological surfaces using the atomic force microscope. *Trends Biotechnol* **17**, 143-150, doi:10.1016/s0167-7799(99)01304-9 (1999).
29 Liu, X. Y. *et al.* Sub-10 nm Resolution Patterning of Pockets for Enzyme Immobilization with Independent Density and Quasi-3D Topography Control. *Acs Appl Mater Inter* **11**, 41780-41790, doi:10.1021/acsami.9b11844 (2019).
30 Albisetti, E. *et al.* Nanopatterning reconfigurable magnetic landscapes via thermally assisted scanning probe lithography. *Nat Nanotechnol* **11**, 545-551 (2016).
31 Howell, S. T., Grushina, A., Holzner, F. & Brugger, J. Thermal scanning probe lithography-a review. *Microsyst Nanoeng* **6**, 21, doi:10.1038/s41378-019-0124-8 (2020).
32 Albisetti, E. *et al.* Thermochemical scanning probe lithography of protein gradients at the nanoscale. *Nanotechnology* **27**, 315302 (2016).
33 Carroll, K. M. *et al.* Fabricating nanoscale chemical gradients with thermochemical nanolithography. *Langmuir* **29**, 8675-8682 (2013).
34 Wang, D. *et al.* Thermochemical Nanolithography of Multifunctional Nanotemplates for Assembling Nano-Objects. *Adv Funct Mater* **19**, 3696-3702 (2009).
35 Tang, S. W. *et al.* Replication of a Tissue Microenvironment by Thermal Scanning Probe Lithography. *Acs Appl Mater Inter* **11**, 18988-18994, doi:10.1021/acsami.9b05553 (2019).
36 Nogues, J. & Schuller, I. K. Exchange bias. *Journal of Magnetism and Magnetic Materials* **192**, 203-232, doi:Doi 10.1016/S0304-8853(98)00266-2 (1999).
37 Adeyeye, A. & Shimon, G. in *Handbook of Surface Science* Vol. 5 1-41 (Elsevier, 2015).
38 Duine, R., Lee, K.-J., Parkin, S. S. & Stiles, M. D. Synthetic antiferromagnetic spintronics. *Nature physics* **14**, 217-219 (2018).
39 Sharma, P. P., Albisetti, E., Monticelli, M., Bertacco, R. & Petti, D. Exchange bias tuning for magnetoresistive sensors by inclusion of non-magnetic impurities. *Sensors* **16**, 1030 (2016).
40 Liu, X., Huang, Z., Zheng, X., Shahrjerdi, D. & Riedo, E. Nanofabrication of graphene field-effect transistors by thermal scanning probe lithography. *APL Materials* **9**, 011107 (2021).

41 Nelson, B. A. & King, W. P. Modeling and simulation of the interface temperature between a heated silicon probe and a substrate. *Nanosc Microsc Therm* **12**, 98-115, doi:10.1080/15567260701866769 (2008).
42 William, P. Parallelization of thermochemical nanolithography. *Nanoscale* **6**, 1299-1304 (2014).
43 Paul, P. C., Knoll, A. W., Holzner, F., Despont, M. & Duerig, U. Rapid turnaround scanning probe nanolithography. *Nanotechnology* **22**, 275306, doi:10.1088/0957-4484/22/27/275306 (2011).
44 Carroll, K. M. *et al.* Fabricating Nanoscale Chemical Gradients with ThermoChemical NanoLithography. *Langmuir* **29**, 8675-8682, doi:10.1021/la400996w (2013).
45 Kazakova, O. *et al.* Frontiers of magnetic force microscopy. *Journal of Applied Physics* **125**, 060901 (2019).
46 Schäfer, R. & McCord, J. in *Magnetic Measurement Techniques for Materials Characterization* 171-229 (Springer, 2021).
47 Fassbender, J. Magnetization dynamics investigated by time-resolved Kerr effect magnetometry. *Spin dynamics in confined magnetic structures II*, 59-92 (2003).
48 Raabe, J. *et al.* PolLux: A new facility for soft x-ray spectromicroscopy at the Swiss Light Source. *Review of scientific instruments* **79**, 113704 (2008).
49 Nan, H. *et al.* Strong photoluminescence enhancement of MoS(2) through defect engineering and oxygen bonding. *ACS Nano* **8**, 5738-5745, doi:10.1021/nn500532f (2014).
50 Parkin, W. M. *et al.* Raman Shifts in Electron-Irradiated Monolayer MoS2. *ACS Nano* **10**, 4134-4142, doi:10.1021/acsnano.5b07388 (2016).
51 Mortelmans, T. *et al.* Grayscale e-beam lithography: Effects of a delayed development for well-controlled 3D patterning. *Microelectron Eng* **225**, doi:ARTN 111272

10.1016/j.mee.2020.111272 (2020).
52 Vieu, C. *et al.* Electron beam lithography: resolution limits and applications. *Appl Surf Sci* **164**, 111-117, doi:Doi 10.1016/S0169-4332(00)00352-4 (2000).
53 Rawlings, C. *et al.* High Throughput Lithography Using Thermal Scanning Probes. *2017 19th International Conference on Solid-State Sensors, Actuators and Microsystems (Transducers)*, 418-422 (2017).
54 Kulmala, T. S. *et al.* Single-nanometer accurate 3D nanoimprint lithography with master templates fabricated by NanoFrazor lithography. *Proc Spie* **10584**, doi:Unsp 1058412

10.1117/12.2305905 (2018).
55 Lassaline, N. *et al.* Optical Fourier surfaces. *Nature* **582**, 506-+, doi:10.1038/s41586-020-2390-x (2020).
56 Skaug, M. J., Schwemmer, C., Fringes, S., Rawlings, C. D. & Knoll, A. W. Nanofluidic rocking Brownian motors. *Science* **359**, 1505-1508, doi:10.1126/science.aal3271 (2018).
57 Zimmermann, S. T., Balkenende, D. W. R., Lavrenova, A., Weder, C. & Brugger, J. Nanopatterning of a Stimuli-Responsive Fluorescent Supramolecular Polymer by Thermal Scanning Probe Lithography. *Acs Appl Mater Inter* **9**, 41454-41461, doi:10.1021/acsami.7b13672 (2017).
58 Finocchio, G., Buttner, F., Tomasello, R., Carpentieri, M. & Klaui, M. Magnetic skyrmions: from fundamental to applications. *Journal of Physics D-Applied Physics* **49**, doi:Artn 423001

10.1088/0022-3727/49/42/423001 (2016).
59 Finocchio, G., Büttner, F., Tomasello, R., Carpentieri, M. & Kläui, M. Magnetic skyrmions: from fundamental to applications. *Journal of Physics D: Applied Physics* **49**, 423001 (2016).
60 Parkin, S. S., Hayashi, M. & Thomas, L. Magnetic domain-wall racetrack memory. *Science* **320**, 190-194 (2008).

61 Torrejon, J. *et al.* Neuromorphic computing with nanoscale spintronic oscillators. *Nature* **547**, 428-431 (2017).
62 Ross, C. A. Patterned magnetic recording media. *Annual Review of Materials Research* **31**, 203-235 (2001).
63 De Teresa, J. M. *et al.* Review of magnetic nanostructures grown by focused electron beam induced deposition (FEBID). *Journal of Physics D-Applied Physics* **49**, doi:Artn 243003

10.1088/0022-3727/49/24/243003 (2016).
64 Williams, G. *et al.* Two-photon lithography for 3D magnetic nanostructure fabrication. *Nano Research* **11**, 845-854, doi:10.1007/s12274-017-1694-0 (2018).
65 Albisetti, E. *et al.* Stabilization and control of topological magnetic solitons via magnetic nanopatterning of exchange bias systems. *Applied Physics Letters* **113**, 162401 (2018).
66 Barman, A. *et al.* The 2021 magnonics roadmap. *Journal of Physics: Condensed Matter* (2021).
67 Pirro, P., Vasyuchka, V. I., Serga, A. A. & Hillebrands, B. Advances in coherent magnonics. *Nature Reviews Materials*, 1-22 (2021).
68 Albisetti, E. *et al.* Optically Inspired Nanomagnonics with Nonreciprocal Spin Waves in Synthetic Antiferromagnets. *Advanced Materials* **32**, doi:ARTN 1906439

10.1002/adma.201906439 (2020).
69 . (!!! INVALID CITATION !!! 16).
70 Liu, X., Howell, S. T., Conde-Rubio, A., Boero, G. & Brugger, J. Thermomechanical nanocutting of 2D materials. *Advanced Materials* **32**, 2001232 (2020).
71 Cheng, B. *et al.* Ultra compact electrochemical metallization cells offering reproducible atomic scale memristive switching. *Communications Physics* **2**, 1-9 (2019).
72 Howland, R. & Benatar, L. *A Practical Guide: To Scanning Probe Microscopy*. (Park scientific instruments, 1996).
73 Lavini, F. *et al.* Friction and work function oscillatory behavior for an even and odd number of layers in polycrystalline MoS2. *Nanoscale* **10**, 8304-8312, doi:10.1039/c8nr00238j (2018).
74 Gao, E. *et al.* Mechanical exfoliation of two-dimensional materials. *Journal of the Mechanics and Physics of Solids* **115**, 248-262 (2018).
75 Liu, Z. *et al.* Strain and structure heterogeneity in MoS 2 atomic layers grown by chemical vapour deposition. *Nature communications* **5**, 1-9 (2014).
76 Holzner, F. *et al.* Directed placement of gold nanorods using a removable template for guided assembly. *Nano Lett* **11**, 3957-3962, doi:10.1021/nl202276q (2011).
77 Balandin, A. A. *et al.* Superior thermal conductivity of single-layer graphene. *Nano letters* **8**, 902-907 (2008).
78 Gandi, A. N. & Schwingenschlögl, U. Thermal conductivity of bulk and monolayer MoS2. *EPL (Europhysics Letters)* **113**, 36002 (2016).
79 Calò, A. *et al.* Spatial mapping of the collagen distribution in human and mouse tissues by force volume atomic force microscopy. *Scientific reports* **10**, 1-12 (2020).
80 Holzner, F. *Thermal scanning probe lithography using polyphthalaldehyde*, ETH Zurich, (2013).
81 Lelek, M. *et al.* Single-molecule localization microscopy. *Nature Reviews Methods Primers* **1**, 1-27 (2021).
82 Withers, P. J. *et al.* X-ray computed tomography. *Nature Reviews Methods Primers* **1**, 1-21 (2021).
83 Holzner, F. *et al.* in *29th European Mask and Lithography Conference.* 888605 (International Society for Optics and Photonics).
84 Ryu Cho, Y. K. *et al.* Sub-10 nanometer feature size in silicon using thermal scanning probe lithography. *ACS nano* **11**, 11890-11897 (2017).

85 Hettler, S. *et al.* Phase masks for electron microscopy fabricated by thermal scanning probe lithography. *Micron* **127**, 102753, doi:10.1016/j.micron.2019.102753 (2019).
86 King, W. P. Design analysis of heated atomic force microscope cantilevers for nanotopography measurements. *Journal of Micromechanics and Microengineering* **15**, 2441 (2005).
87 Burch, K. S., Mandrus, D. & Park, J.-G. Magnetism in two-dimensional van der Waals materials. *Nature* **563**, 47-52 (2018).
88 Jungwirth, T., Marti, X., Wadley, P. & Wunderlich, J. Antiferromagnetic spintronics. *Nat Nanotechnol* **11**, 231-241 (2016).